Supporting Information

Riboglow: a multicolor riboswitch-based platform for live cell imaging of mRNA and small non-coding RNA in mammalian cells

Supplementary Figures

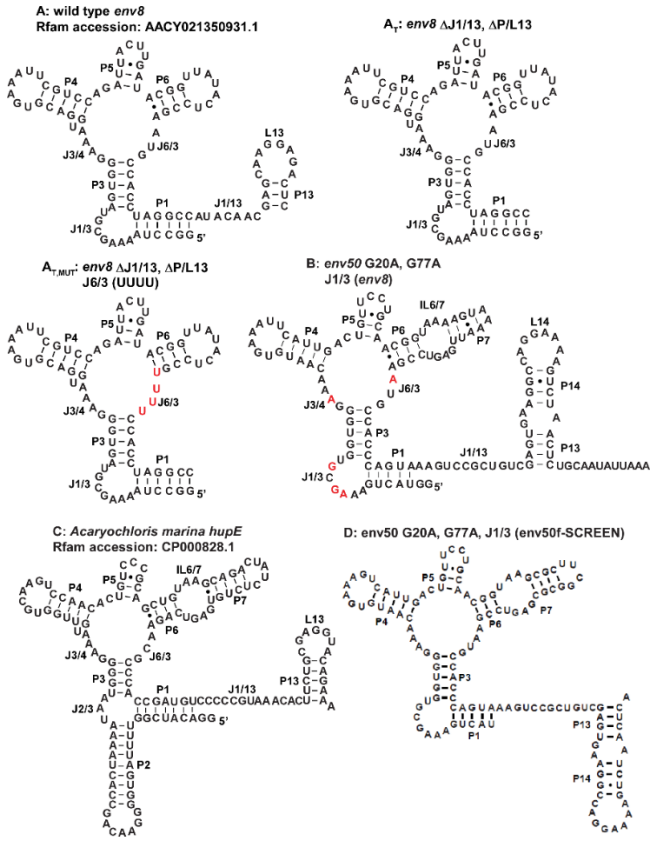

Supplementary Figure 1

Secondary structures of RNAs used in this study with key structural regions denoted as P (paired), J (junction), L (loop), and IL (internal loop). Naturally derived sequences are shown with accompanying Rfam accession numbers, and the secondary structure of wild type *env8* (variant A) is based on crystallographic data[1]. Nucleotides that are colored red in variant $A_{T,MUT}$ represent point mutations made to the binding core of wild type *env8* that abrogate cobalamin binding. Nucleotides that are colored red in variant B represent point mutations derived from wild type *env8* that have been shown to increase the affinity of this RNA[2] for forms of cobalamin similar to the conjugates used in this study. Features that induce bulkiness of the RNA include P13 for variant A, P7, P13, P14 for variant B and P7, P2, P13 for variant C. Variant D is an L4 and P7-optimized variant B that improved cobalamin affinity (data not published prior to this study, see also Supplementary Fig. 8).

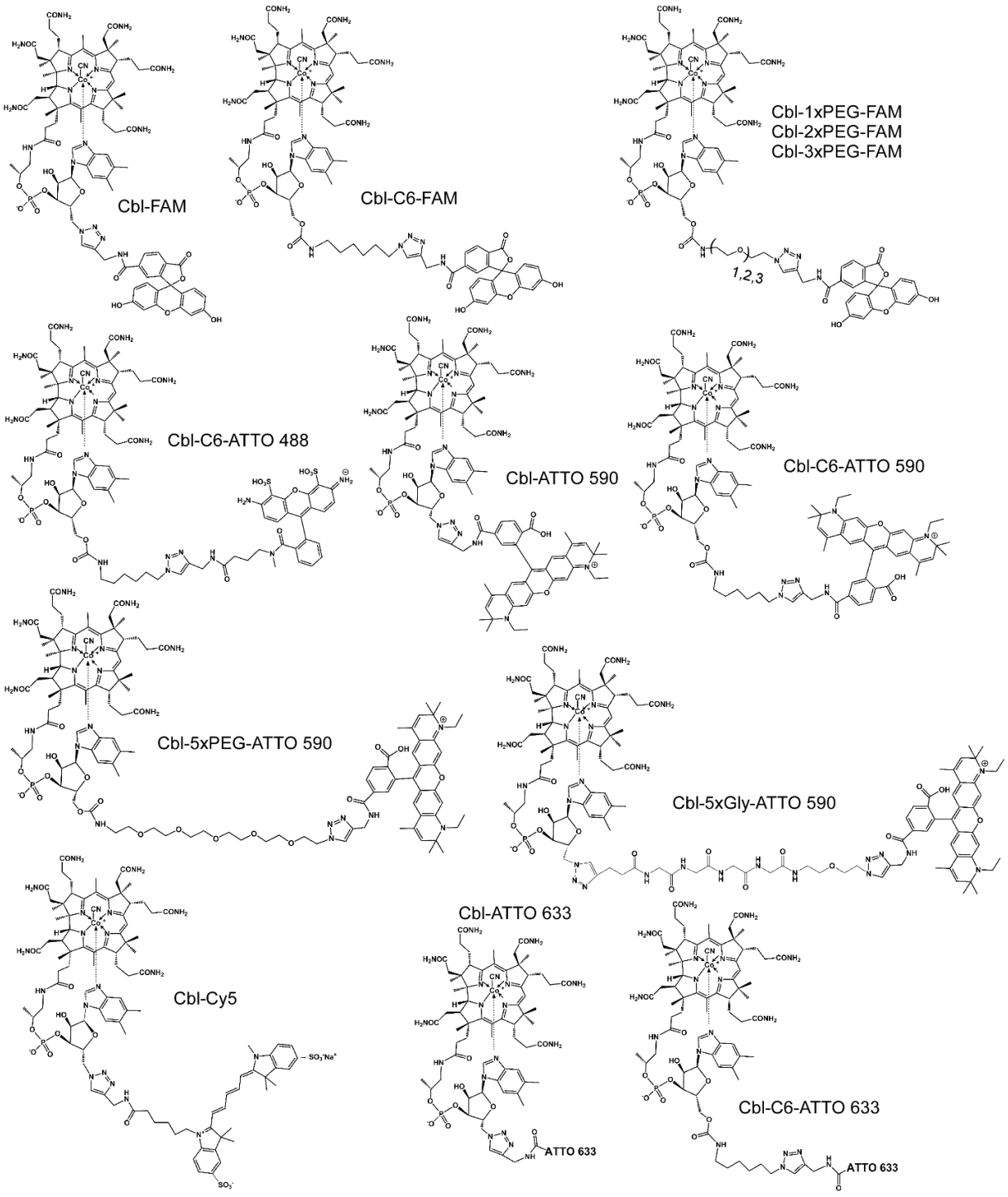

Supplementary Figure 2

Chemical structures of probes used in this study. Note that the chemical structure of the ATTO 633 dye is proprietary and unknown.

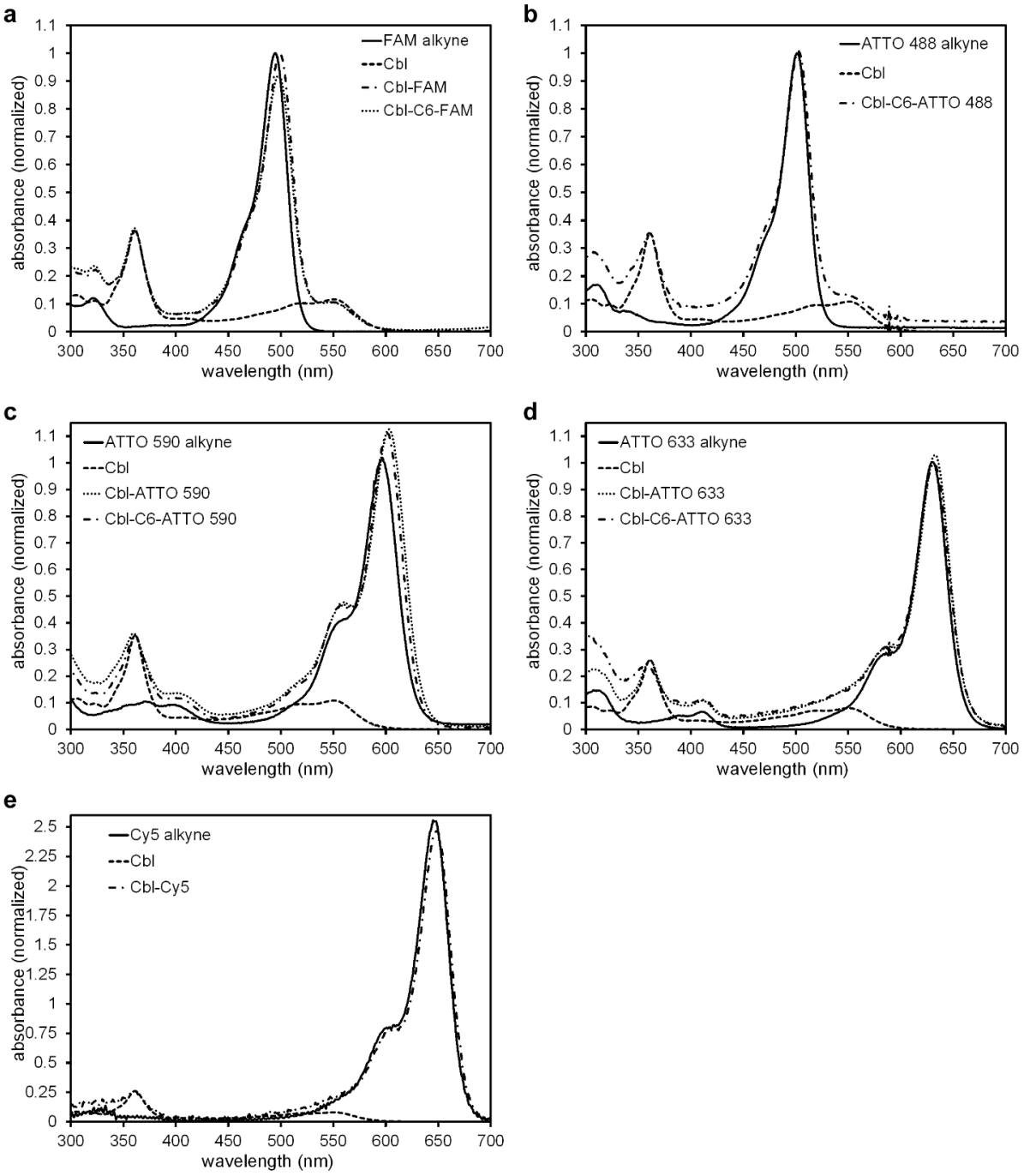

Supplementary Figure 3

Absorbance spectra of representative Cbl-fluorophore probes in comparison to the spectra of free Cbl and each fluorophore. The absorbance intensities were normalized to the maximum absorbance peak of Cbl at 361 nm to allow for evaluation of changes in absorbance peak shapes.

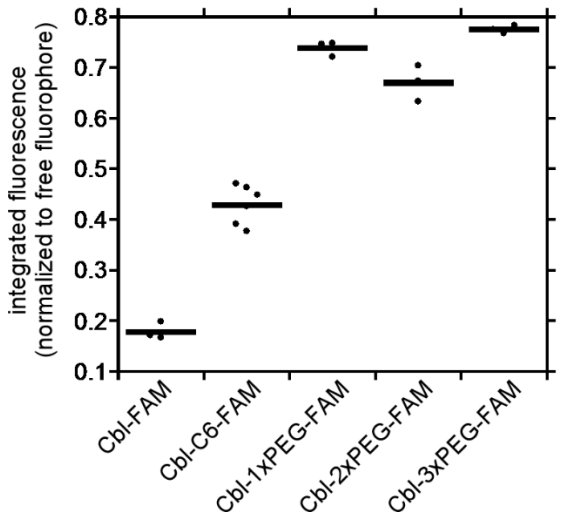

Supplementary Figure 4

Comparison of residual fluorescence for Cbl-FAM probes with varied linkers. The fluorescence was quantified and compared to the signal of the free fluorophore at the same concentration as in Figure 1d. The mean for at least n = 3 independent measurements is shown.

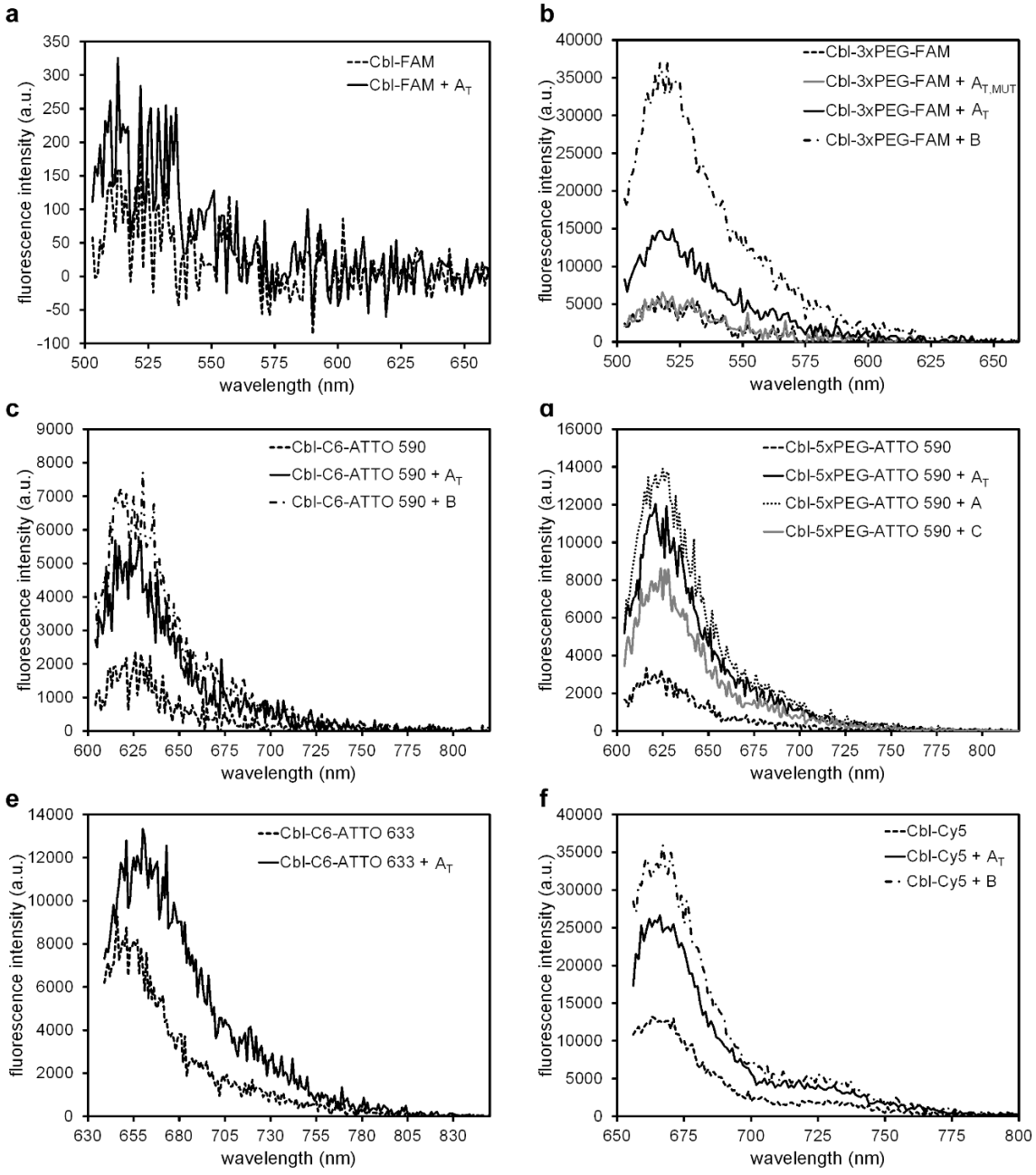

Supplementary Figure 5

Representative fluorescence spectra of Cbl-fluorophore probes in the presence and absence of RNAs used in this study (see also Supplementary Table 1 for photophysical properties). Spectra show an increase in fluorescence intensity upon binding RNAs A, A_T, B, or C but not the non-binding variant $A_{T,MUT}$. Triplicates of spectra shown here were used to generate the bar graphs presented in Figure 2.

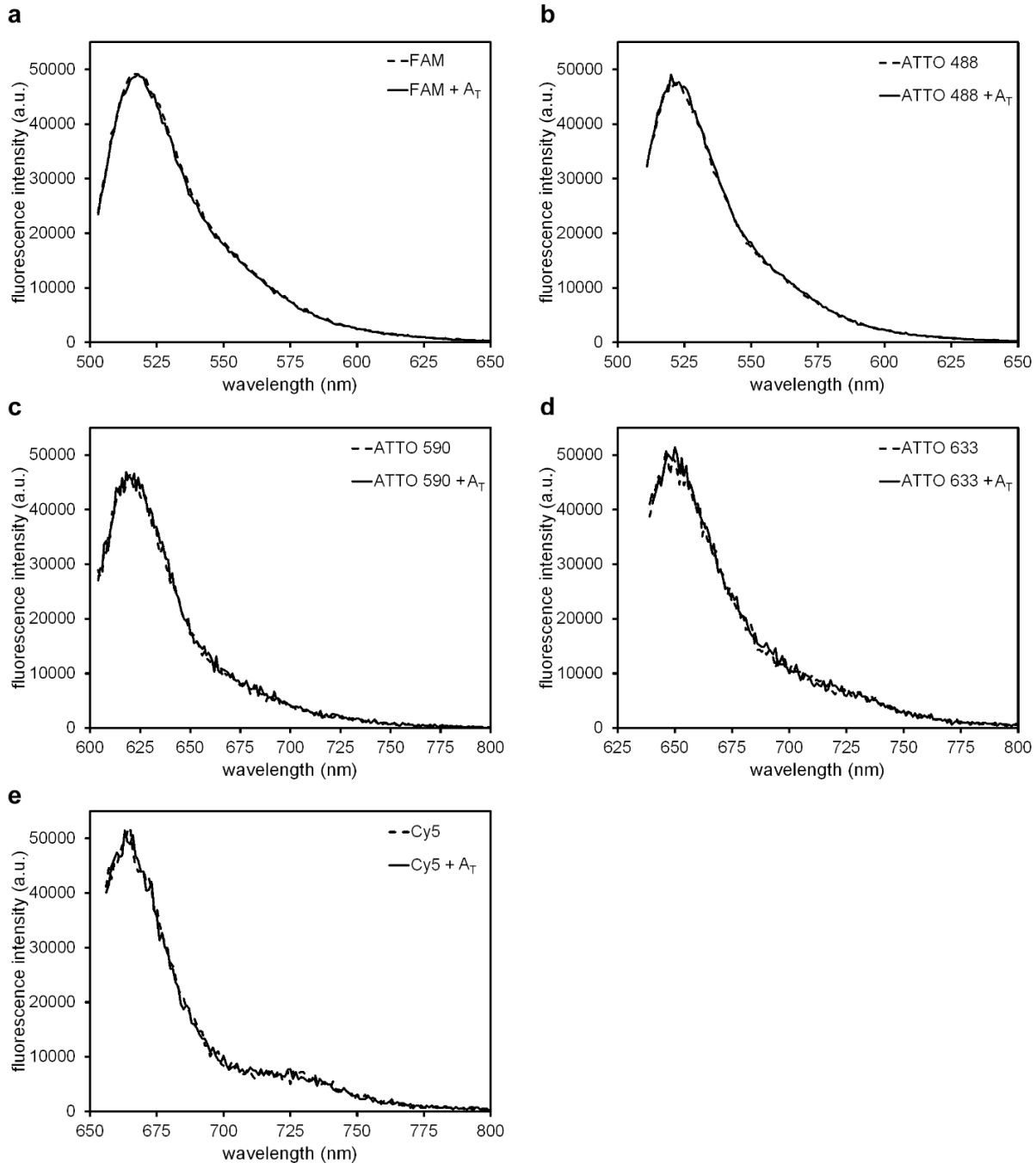

Supplementary Figure 6

Representative fluorescence spectra of free fluorophores used in this study in the presence and absence of RNA variant A_T. Spectra reveal no change in fluorescence intensity of free fluorophores in the presence of A_T. Triplicates of spectra shown here were used to generate the bar graphs presented in Figure 1.

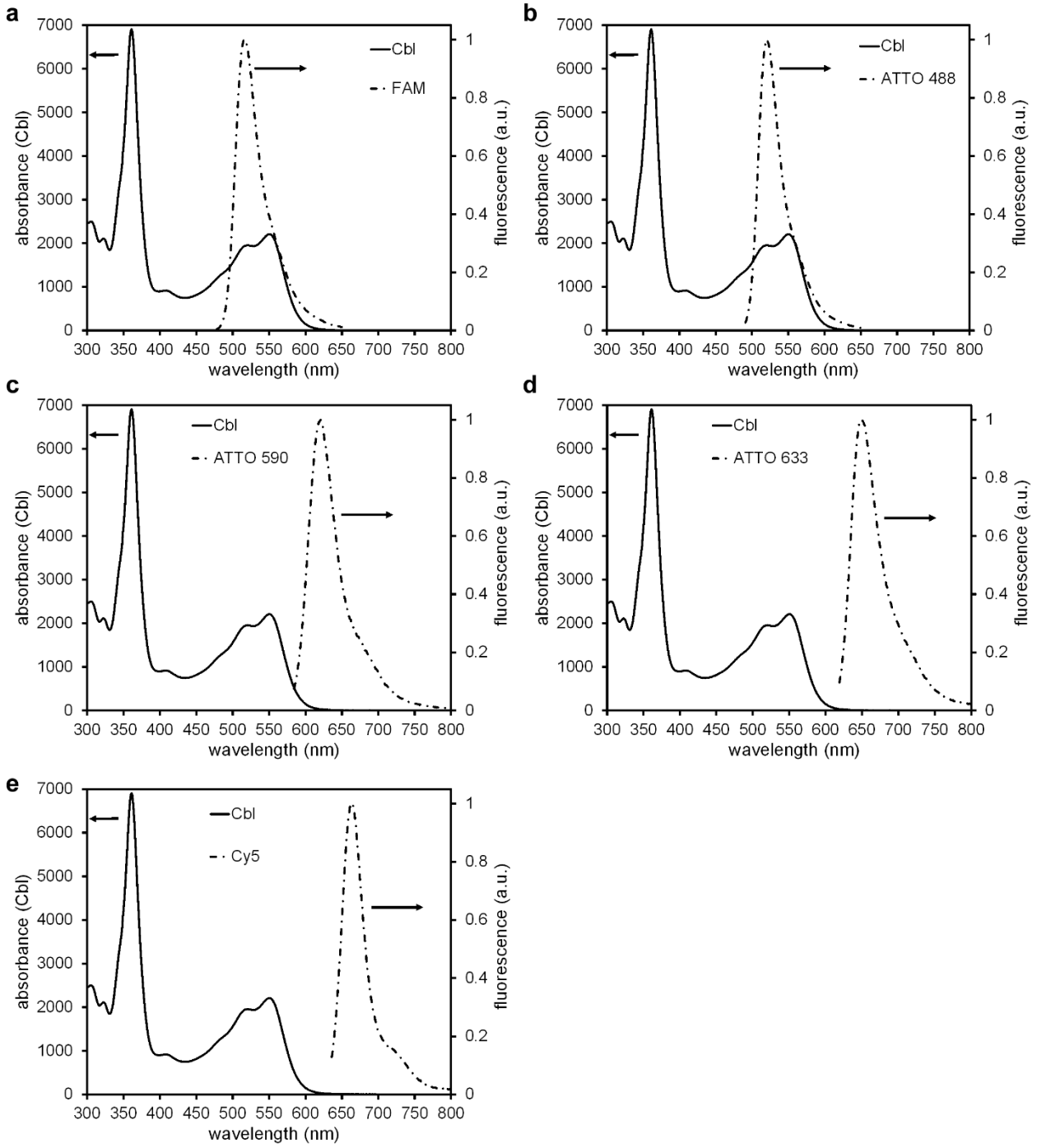

Supplementary Figure 7

Cbl absorbance spectra and fluorescence emission spectra of fluorophores to calculate the overlap integral J(λ). Arrows assign y axis for the indicated spectra.

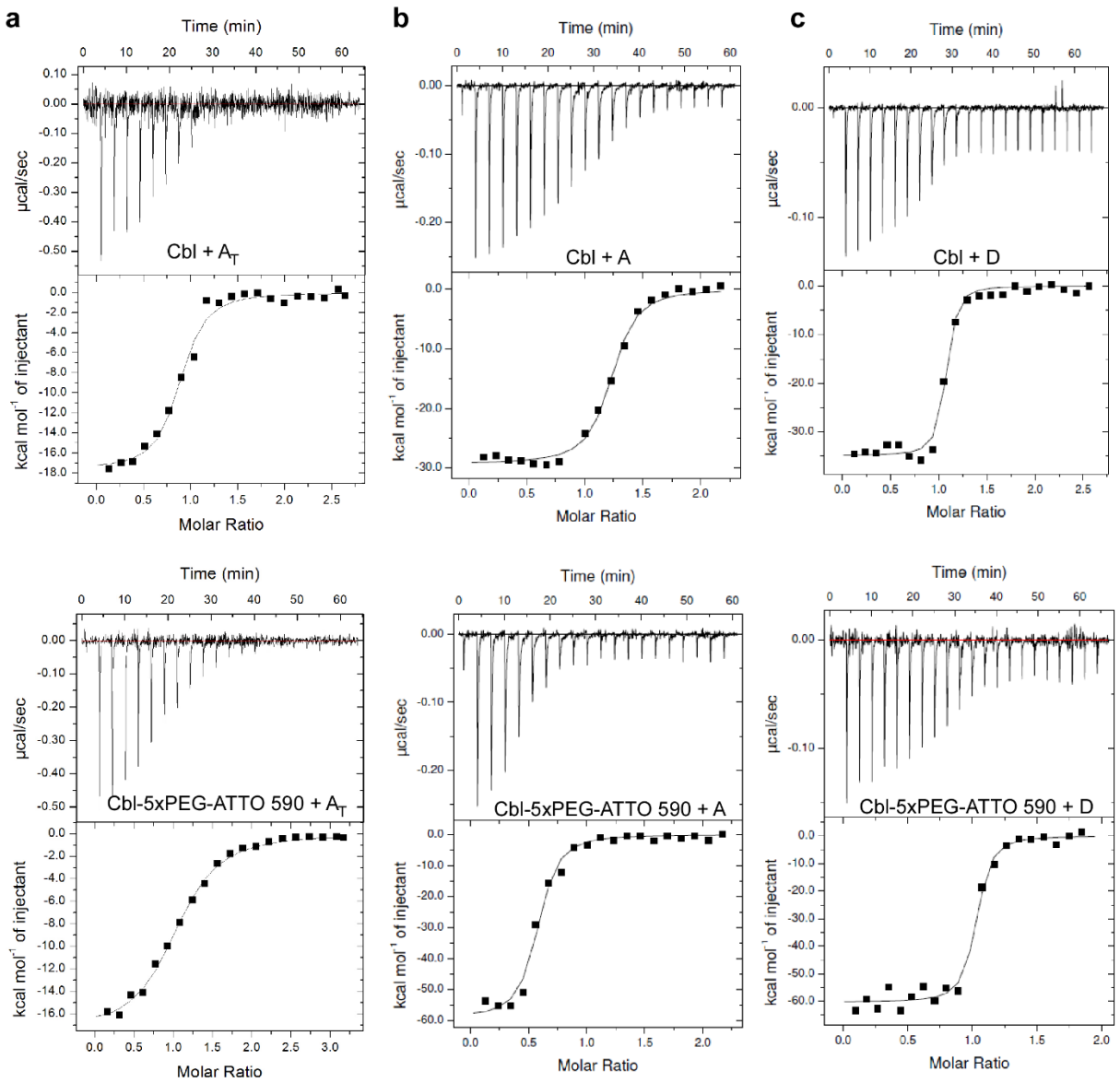

Supplementary Figure 8

RNA variants A and D (panels b and c), but not A_T (panel a), bind to the probe Cbl-5xPEG-ATTO 590 with a dissociation constant (K_D) in the nM range. Representative isothermal titration calorimetry thermograms of the RNA binding to Cbl (top) and Cbl-5xPEG-ATTO 590 (bottom) are presented. K_D values as the mean of 3 independent experiments +/- STDEV are listed in Supplementary Table 6.

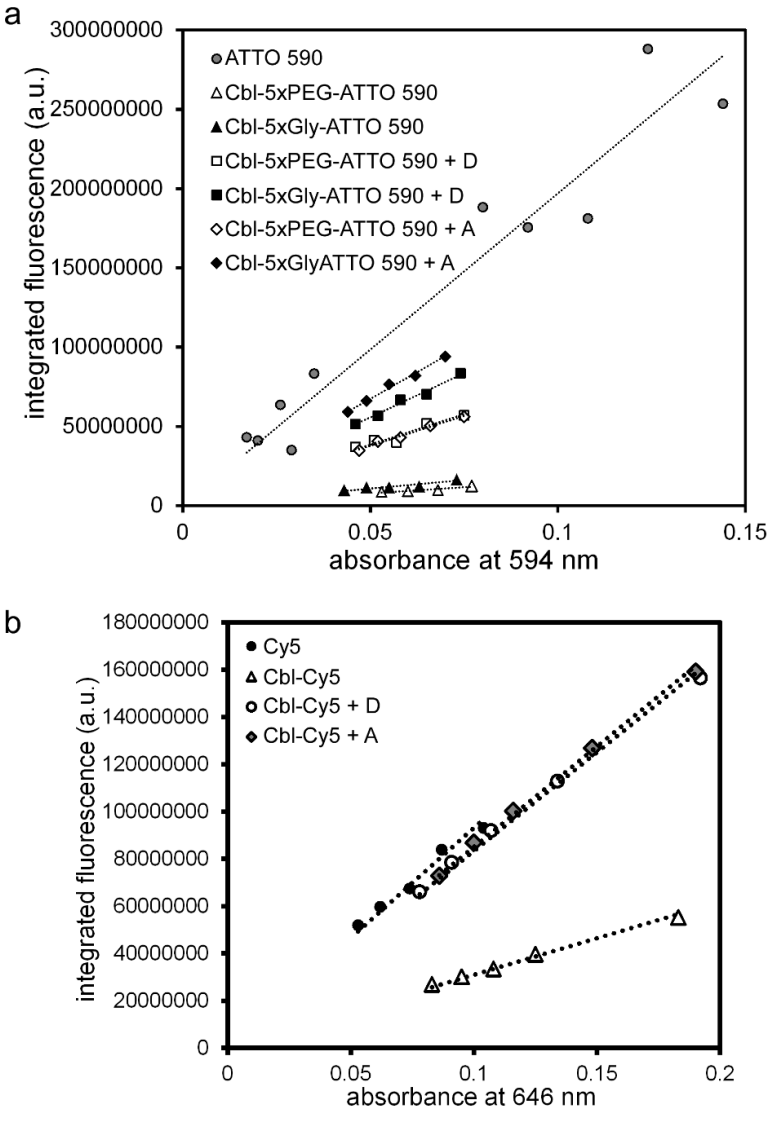

Supplementary Figure 9

Determination of the quantum yield for different Cbl-fluorophore probes in the presence and absence of various RNAs. (a) The quantum yield for ATTO 590 conjugates Cbl-5xPEG-ATTO 590 and Cbl-5xGly-ATTO590 in the presence and absence of variants A and D was measured using ATTO 590 as a reference. (b) The quantum yield for Cbl-Cy5 in the presence and absence of variants A and D was measured using Cy5 as a reference. The absorbance and integrated fluorescence sample was measured for samples of a dilution series of the indicated samples.

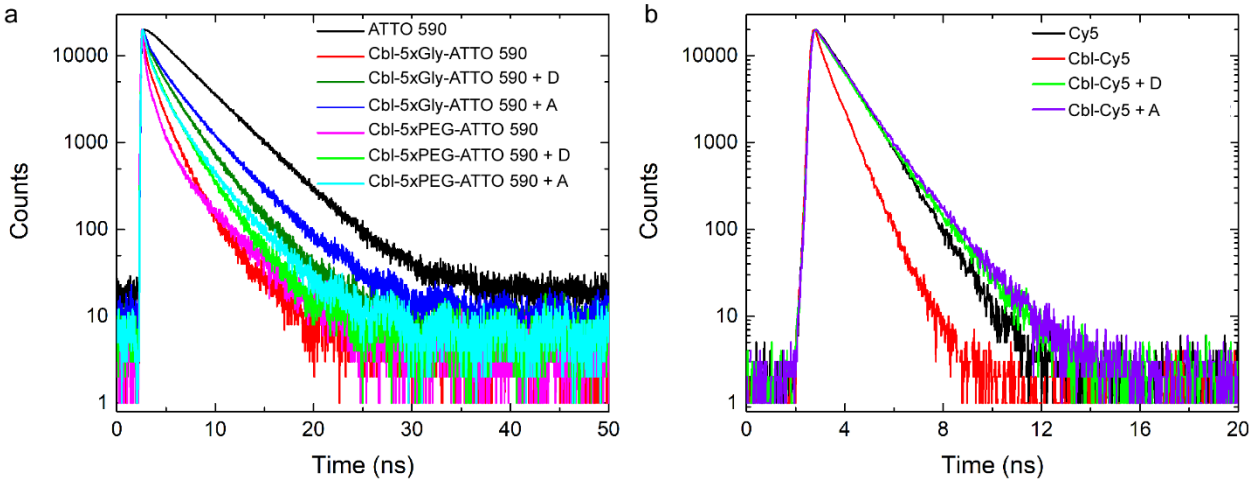

Supplementary Figure 10

Measurement of fluorescence lifetime of Cbl-fluorophore probes in the presence and absence of RNA. (a) The fluorescence lifetime of 0.5 μM Cbl-5xGly-ATTO 590 and Cbl-5xPEG-ATTO 590 in the presence and absence of 5 μM of RNA variants A or D was measured in comparison to 0.5 μM free ATTO 590. (b) The fluorescence lifetime of 0.5 μM Cbl-Cy5 in the presence and absence of 5 μM of RNA variant A or D was measured in comparison to 0.5 μM free Cy5.

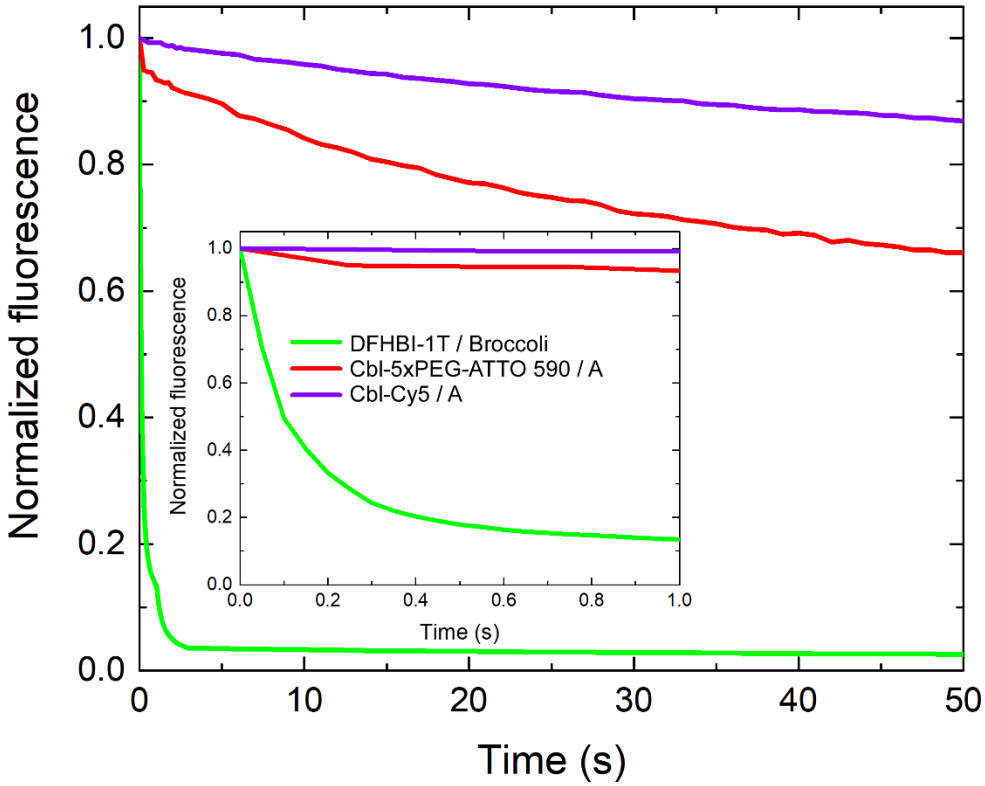

Supplementary Figure 11

Photobleaching of RNA / probe complexes. Droplets containing the indicated RNA / probe complexes were constantly illuminated on a widefield microscope. The excitation rate (the number of absorbed excitation photons, determined from the extinction coefficient) were the same for each sample (see Supplementary Table 9 for a summary of experimental conditions). Representative background subtracted and normalized fluorescence decay curves for each sample are reported. Inset: Photobleaching for the first 1 s.

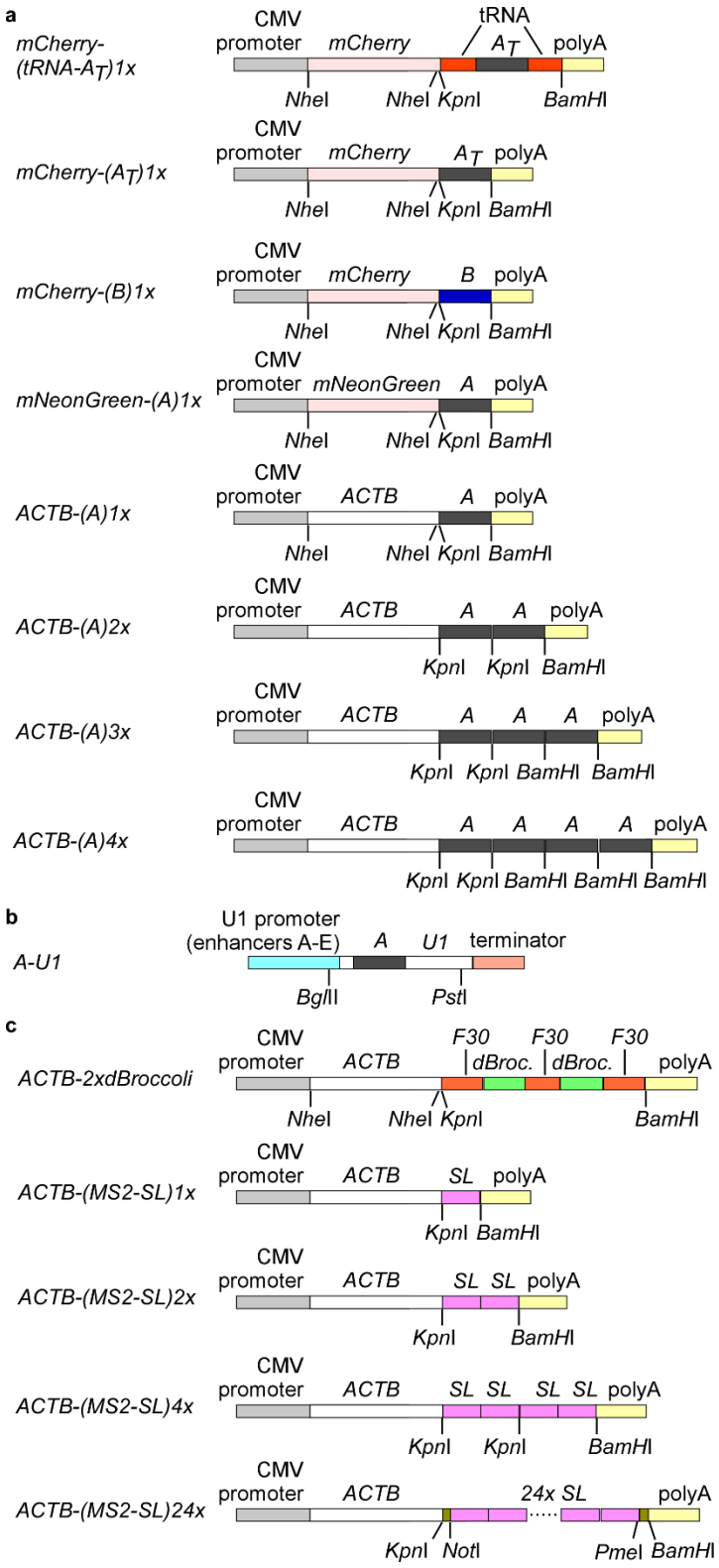

Supplementary Figure 12

Plasmid maps of RNA fusion constructs used in this study.

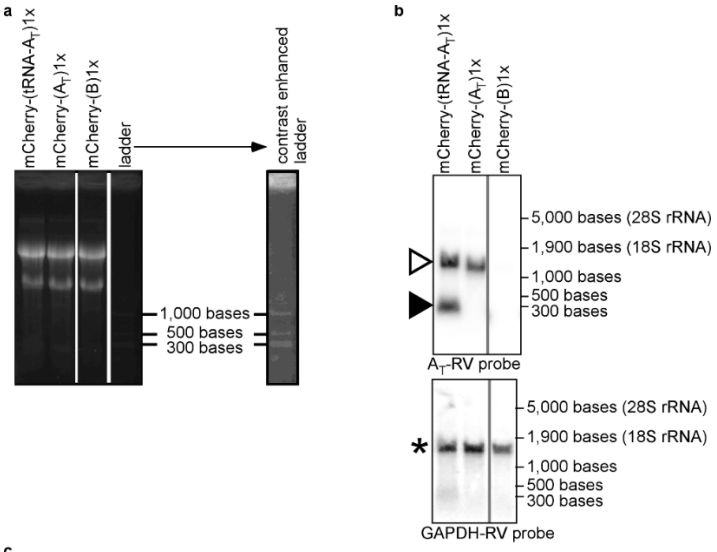

c

Name	Sequence	Melting temperature (IDT)
A_T- RV	5'-CGC GGG GCC TAG GTG-3'	59.4°C
GAPDH-RV	5'-GGC ATG GAC TGT GGT CAT GAG-3'	58.1°C

Supplementary Figure 13

mRNA can be tagged with RNA variant A_T without unwanted processing. 293T cells were transiently transfected with plasmid DNA where the A_T or B tag was genetically fused to a reporter mRNA (encoding mCherry). The tag A_T was produced with or without the tRNA folding scaffold. (a) Total RNA was separated by agarose gel electrophoresis. The 28*S* and 18*S* rRNA bands across samples serve as loading controls and indicate that no unwanted RNA processing occurred during RNA preparation. Non-consecutive lanes of the same gel are indicated by vertical lines. Contrast settings were identical for all parts of the gel. A contrast enhanced version of the lane with the RNA ladder is shown as a reference. (b) Northern blot probed against A_T (top panel) indicates that the full length mRNA (open triangle) is processed when produced with the tRNA folding scaffold (filled triangle). The blot was stripped and probed for GAPDH mRNA (star in bottom panel). Non-consecutive lanes of the same blot are indicated by vertical lines. No changes were made to contrast settings after cropping lanes. (c) Properties of oligonucleotides from (b). The tRNA processing phenotype was reproducible for two independent experiments.

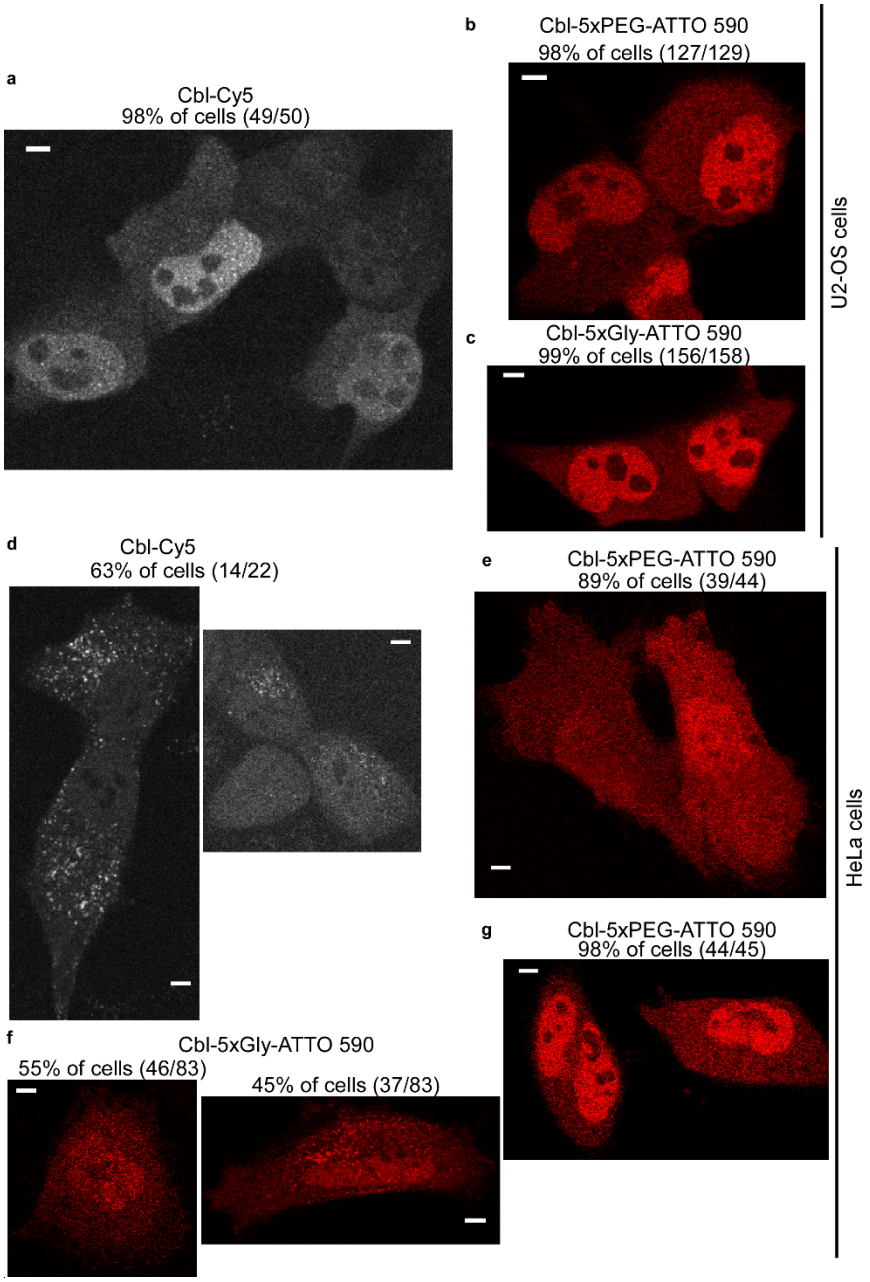

Supplementary Figure 14

Residual fluorescence of Cbl-fluorophore probes reports on probe localization in live cells upon bead loading. (a) Bead loading of Cbl-Cy5 in U2-OS Halo-G3BP1 cells results in diffuse cytosolic and nuclear probe localization with negligible probe aggregation (1 experiment, 50 cells). (b) Cbl-5xPEG-ATTO 590 loaded in U2-OS Halo-G3BP1 cells localizes diffusely in the cytosol and nucleus (1 experiment, 129 cells). (c) Cbl-5xGly-ATTO 590 localizes diffusely in the

cytosol and nucleus of U2-OS Halo-G3BP1 cells (1 experiment, 158 cells). (d) Bead loading of Cbl-Cy5 in HeLa cells results in substantial localization of the Cbl-Cy5 probe in puncta (63% of cells, 1 experiment, 22 cells). (e) Cbl-5xPEG-ATTO 590 loaded in HeLa cells is largely localized diffusely in the nucleus and cytosol (89% of cells, 1 experiment, n = 44 cells). (f) In about half of HeLa cells loaded with Cbl-5xGly-ATTO 590 the probe localized in puncta in the cytosol (45% of cells, 1 experiment, 83 cells). (g) Increasing the concentration of Cbl-5xPEG-ATTO 590 when loading HeLa cells does not alter diffuse cytosolic and nuclear localization of the probe (1 experiment, 45 cells). Compare localization of loading 50 μM probe in (g) versus 0.5 μM probe in (e). Scale bar = 5 μm.

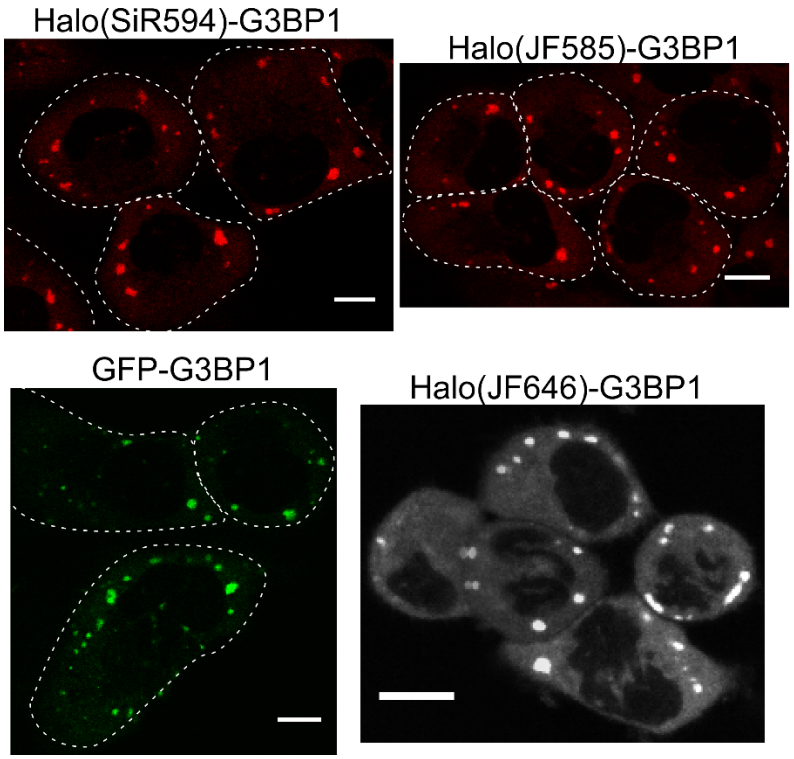

Supplementary Figure 15

Stress granule (SG) visualization by Halo-tag or GFP in U2-OS cells. Top panel: U2-OS cells producing Halo-tagged G3BP1 from the chromosome were treated with two different red fluorescent Halo dyes (SiR594 and JF585). Arsenite stress induced recruitment of Halo-G3BP1 to SGs. Bottom panel, left: U2-OS cells stably producing GFP-G3BP1 were treated with arsenite to induce SGs. Bottom panel, right: U2-OS cells producing Halo-tagged G3BP1 from the chromosome were treated with a far red fluorescent Halo dye (JF646). Scale bar = 10 μm.

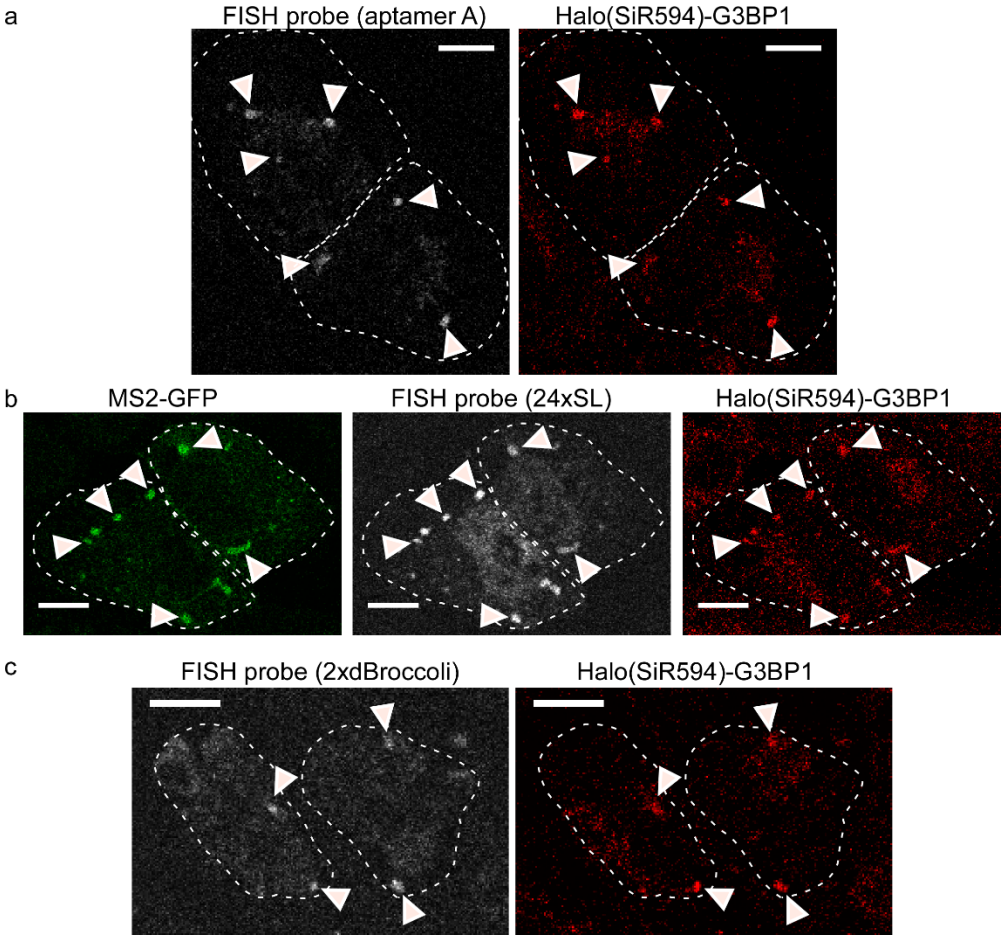

Supplementary Figure 16

ACTB mRNA fused with different RNA visualization tags localizes to stress granules (SG). Plasmids encoding for ACTB tagged with RNA visualization tags at the 3' end were transfected in U2-OS Halo-G3BP1 cells. G3BP1 was labeled with red fluorescent SiR594 dye 24 h post transfection and SGs were induced by treatment with arsenite for 30-45 min. Cells were fixed, permeabilized and the RNA tag was probed with Cy5-fluorescently labeled oligos against the indicated RNA tag. (a) transfection with ACTB-(A)4x (1 experiment, 15 cells) (FISH probe: A_T-FISH-Cy5); (b) transfection with ACTB-(MS2-SL)24x (1 experiment, 8 cells) (FISH probe: MS2SL-FISH-Cy5); (c) transfection with ACTB-2xdBroccoli (1 experiment, 13 cells) (FISH probe: Broccoli-FISH-Cy5). Scale bar = 10 μm.

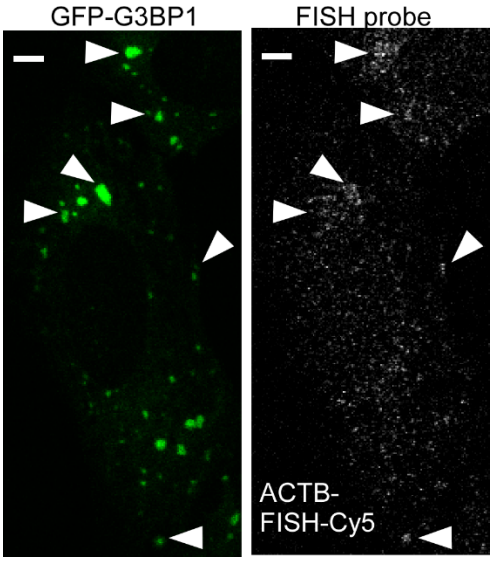

Supplementary Figure 17

Endogenous ACTB mRNA colocalizes with GFP-G3BP1, a marker protein for SGs in U2-OS cells. Detection of endogenous ACTB mRNA in U2-OS cells that stably produce GFP-G3BP1, a SG marker protein. Cells were fixed, permeabilized and ACTB fusion mRNA was visualized by FISH using a Cy5-conjugated probe. Representative cells show localization of ACTB mRNA to SGs (1 experiment, 15 cells). Scale bar = 5 μm.

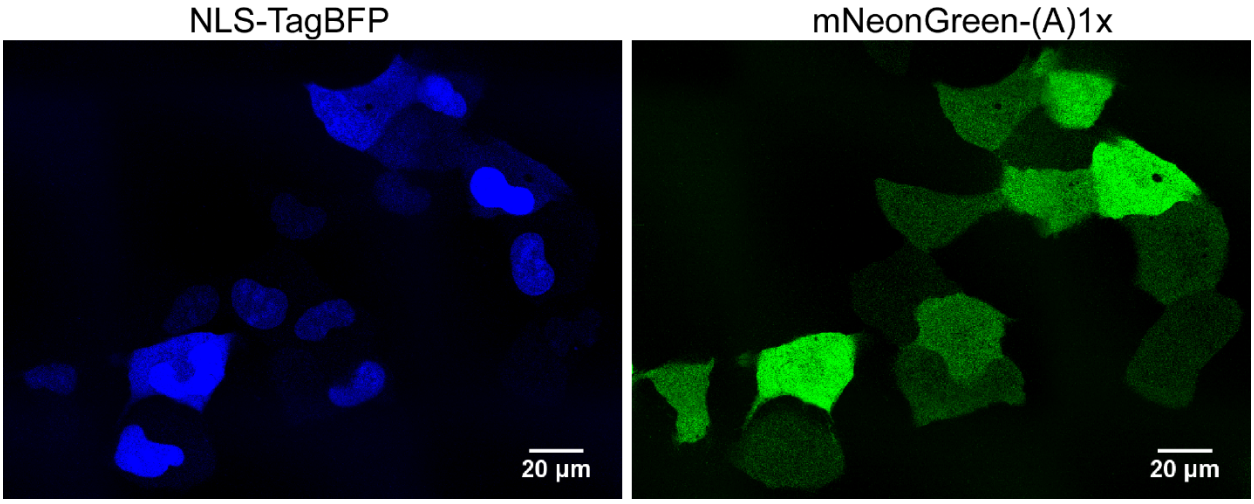

Supplementary Figure 18

Transfecting U2-OS cells with the plasmid NLS-TagBFP serves as a transfection marker for mRNA-tagged plasmids. U2-OS cells were transfected with a 1:1 mixture of NLS-TagBFP and mNeonGreen-(A)1x and the fluorescence signal was analyzed 24 h post transfection. Each cell harboring the blue NLS-TagBFP transfection marker was assessed for presence of green fluorescence as a measure for successful transfection of mNeonGreen mRNA tagged with riboswitch variant A. 94% of cells with NLS-TagBFP also have mNeonGreen signal (2 independent experiments, 561 cells).

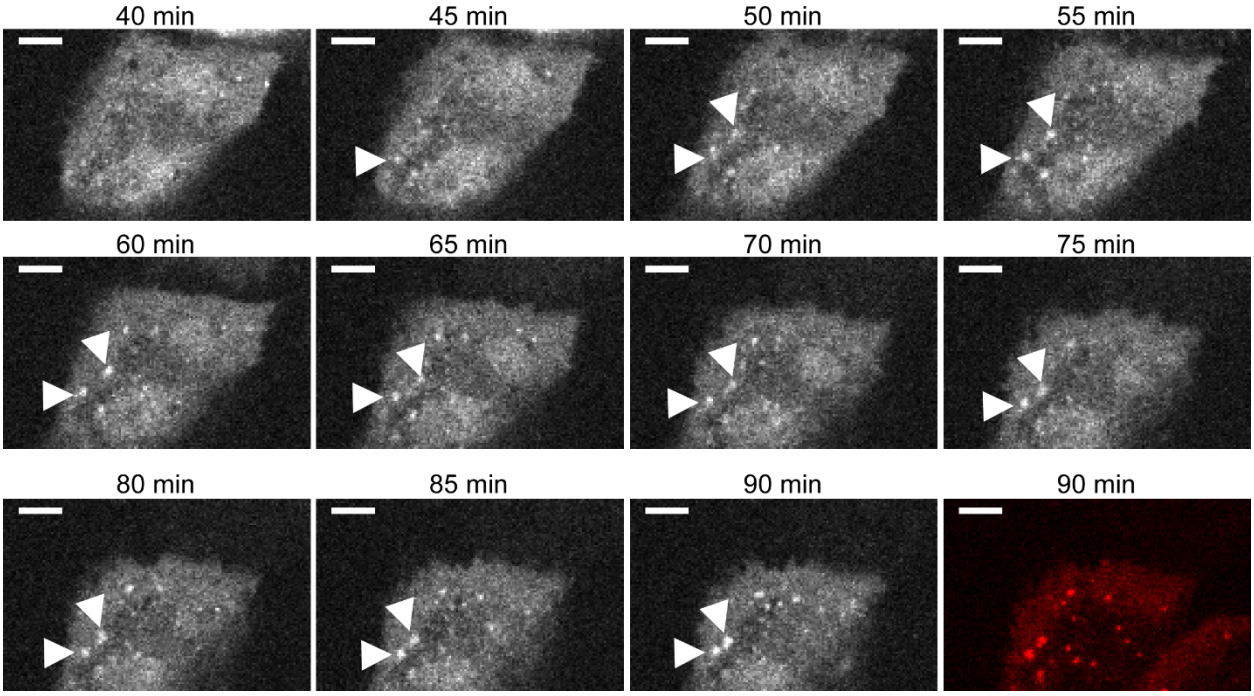

Supplementary Figure 19

Time course of ACTB mRNA recruitment to stress granules (SG) and dynamics of SGs. U2-OS cells constitutively producing Halo-G3BP1 were transfected with a plasmid to produce ACTB-(A)4x mRNA and a transfection marker (NLS-TagBFP) as in Fig. 3. 24 h post transfection, cells were stained with the JF585 Halo dye, bead loaded with Cbl-Cy5 and treated with 0.5 mM arsenite to induce SGs. Shown are fluorescence images in the Cbl-Cy5 channel (collected in 5 min intervals). Cbl-Cy5 labels ACTB-(A)4x mRNA and formation of SGs is visible at about 45 min post arsenite treatment (white arrows). SGs move throughout the cell and are closer together by 90 min post arsenite treatment (white arrows). Red panel: 90 min time point collected in the red fluorescence channel to visualize Halo-G3BP1 via the JF585 dye. Scale bar = 5 µm.

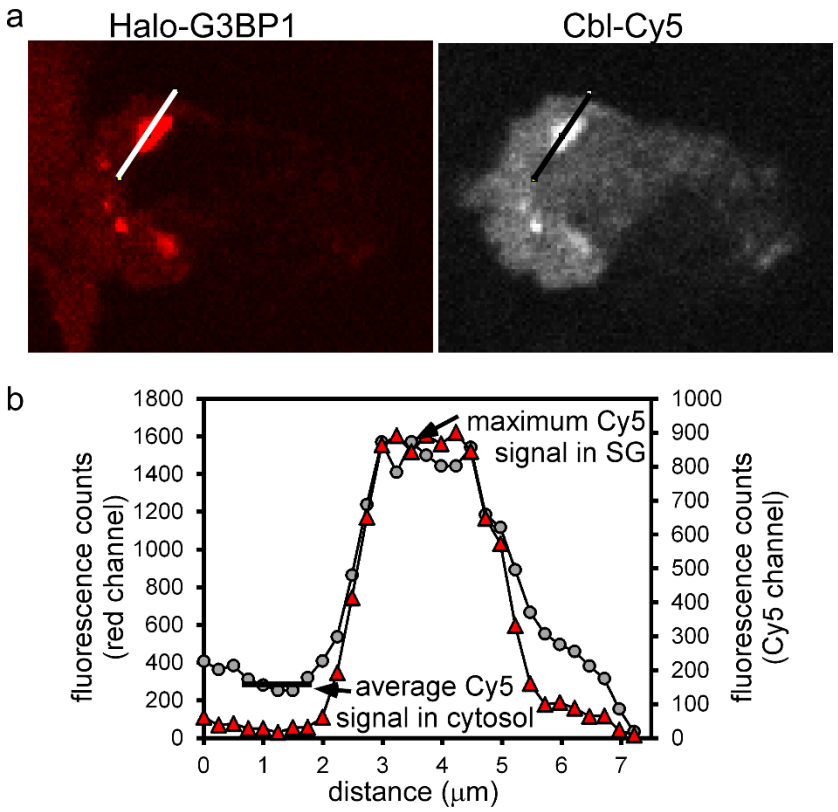

Supplementary Figure 20

Analysis of live U2-OS cells to quantify Cbl-fluorophore probe fluorescence in stress granules (SG). (a) SGs were identified in the Halo-G3BP1 channel via labeling of G3BP1 with JF585 and a line trace was drawn through the SG including cytosolic fluorescence near the SG. The same signal trace was recorded in the probe fluorescence channel (shown here for Cbl-Cy5). (b) After background subtraction, the Cbl-fluorophore probe fluorescence trace as well as the control Halo-G3BP1 trace were plotted. The maximum fluorescence signal for the Cbl-fluorophore probe was determined and divided by the average probe fluorescence in the cytosol.

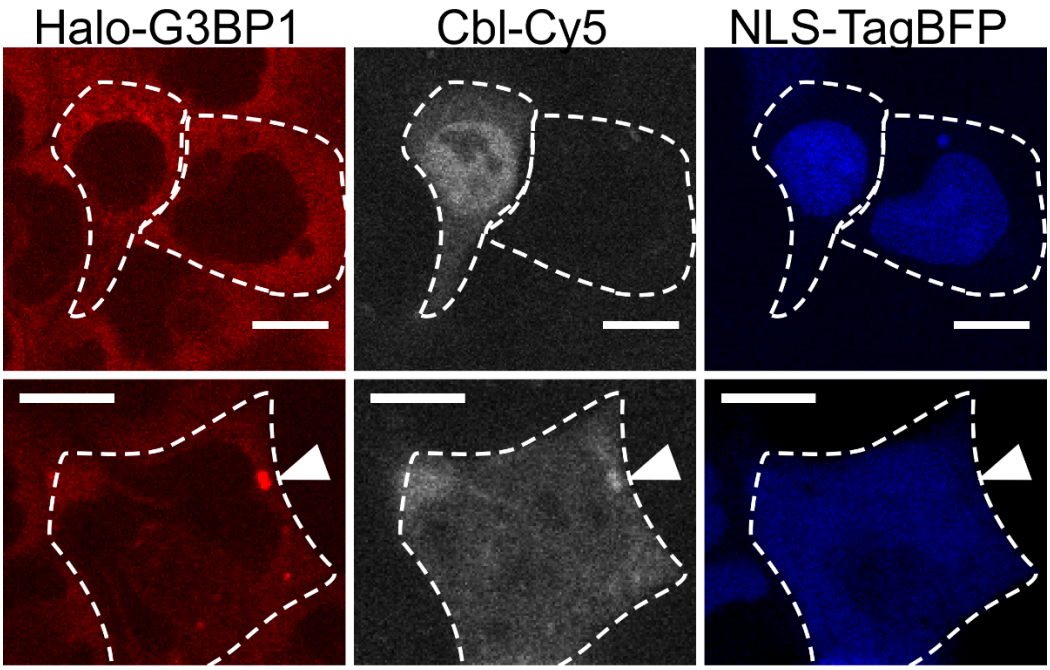

Supplementary Figure 21

Localization phenotypes for U2-OS cells transfected with tagged mRNA and loaded with Cbl-Cy5 probe in the absence of arsenite stress. U2-OS cells producing Halo-G3BP1 from the genome were transfected with the plasmid ACTB-(A)4x and the transfection marker plasmid NLS-TagBFP as in Fig. 3. Halo-G3BP1 was labeled with JF585 24 h post transfection and Cbl-Cy5 was bead loaded. Shown are representative cells demonstrating two different phenotypes. Top panel: Halo-G3BP1 was diffusely localized in the cytosol and Cbl-Cy5 displayed nuclear and cytosolic localization as in the untransfected control Fig. 3c). Bottom panel: In some cells, stress granules (SGs) formed in the absence of arsenite treatment, as indicated by the signal in the red Halo-G3BP1 channel. The process of transfection has been shown to lead to formation of SGs in a small number of cells. In the cell shown here, Cbl-Cy5 fluorescence colocalized with SGs (white arrow), as expected due to recruitment of ACTB tagged with the RNA tag variant A to SGs. 2 experiments, 20 cells positive for Cbl-Cy5 and NLS-TagBFP (12 cells without SGs in red channel, 8 cells with SGs in red channel). Scale bar = 10 μm.

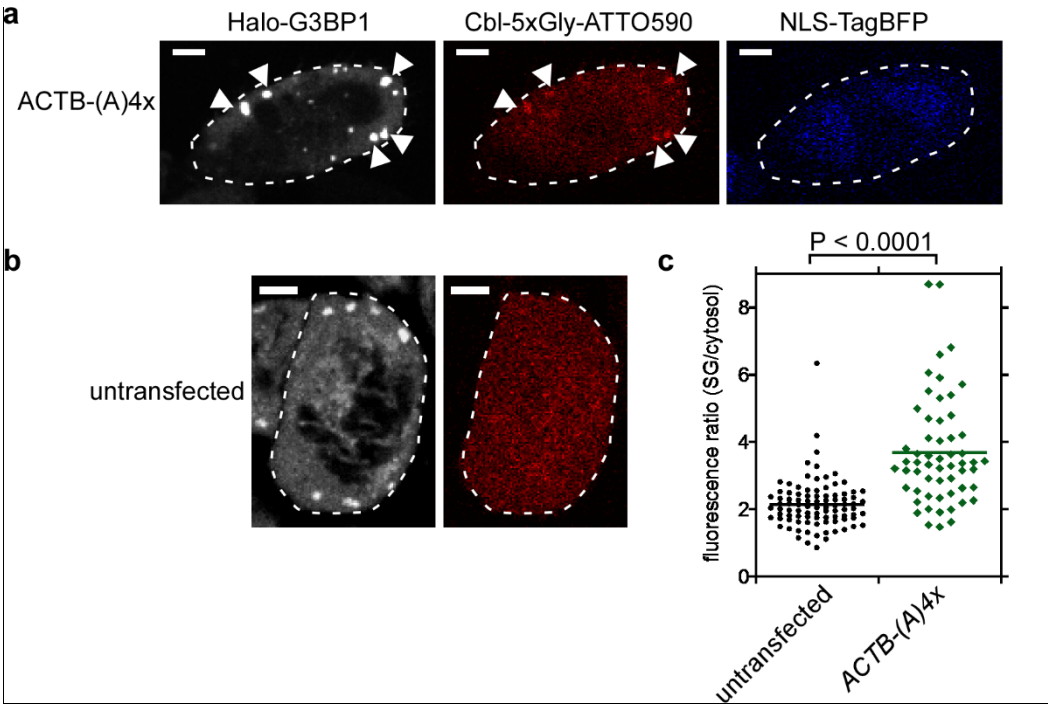

Supplementary Figure 22

Cbl-5xGly-ATTO590 fluorescence signal increased in SGs in cells that were transiently transfected with ACTB-(A)4x. (a) U2-OS cells producing Halo-G3BP1 were transfected with ACTB-(A)4x and the transfection marker TagBFP. 24 h post transfection, cells were stained with the JF646 Halo dye. The probe Cbl-5xGly-ATTO590 was introduced into cells by bead loading, SG formation was induced by treatment with 0.5 mM arsenite for 45 min, followed by live cell microscopy (2 experiments, 22 cells, 59 SGs). In 64% of the cells at least one SG was detectable and 58% of all SGs were detected in the Cbl-5xGly-ATTO 590 channel. (b) The same experiment as in (a) was performed, except that ACTB-(A)4x was not transfected (2 experiments, 37 cells, 92 SGs). In 0% of the cells at least one SG was detectable and 0% of all SGs were detected in the Cbl-5xGly-ATTO 590 channel. (c) Fluorescence increase for Cbl-5xGly-ATTO590 in SGs was quantified by collecting a line trace through each SG (identified in the JF646 channel) and calculating the ratio of the highest signal in the SG over the average signal in the cytosol (see Supplementary Figure 20 for details). One way ANOVA (95% confidence limit), post hoc test (Tuskey HSD), scale bar = 10 μm.

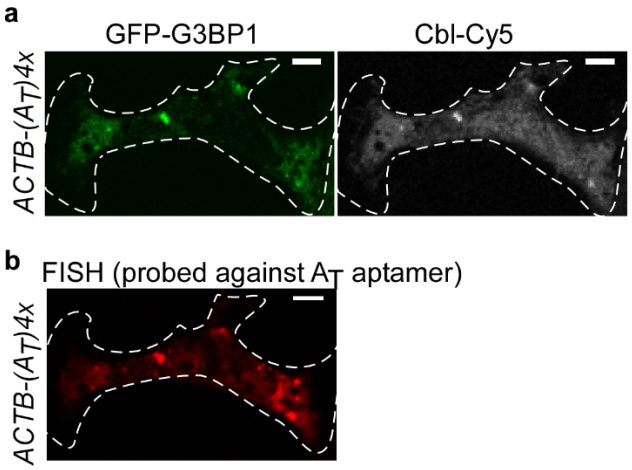

Supplementary Figure 23

Correlative fluorescence microscopy of live (a) and fixed cells (b) confirms colocalization of ACTB mRNA to SGs. U2-OS cells that stably produce GFP-G3BP1 were transfected with a plasmid encoding for ACTB-(A_T)4x. 24 h post transfection, the probe Cbl-Cy5 was loaded and SGs were induced by arsenite treatment. After live imaging, cells were fixed, permeabilized and probed with a FISH probe against the A_T tag. (a) Fluorescence of Cbl-Cy5 colocalized with SGs. (b) After fixation, localization of the A_T tag to SGs was directly assessed by a red fluorescent (Alexa546) FISH probe (A_T-FISH-Alexa546) (2 experiments, 4 cells). Scale bar = 5 μm.

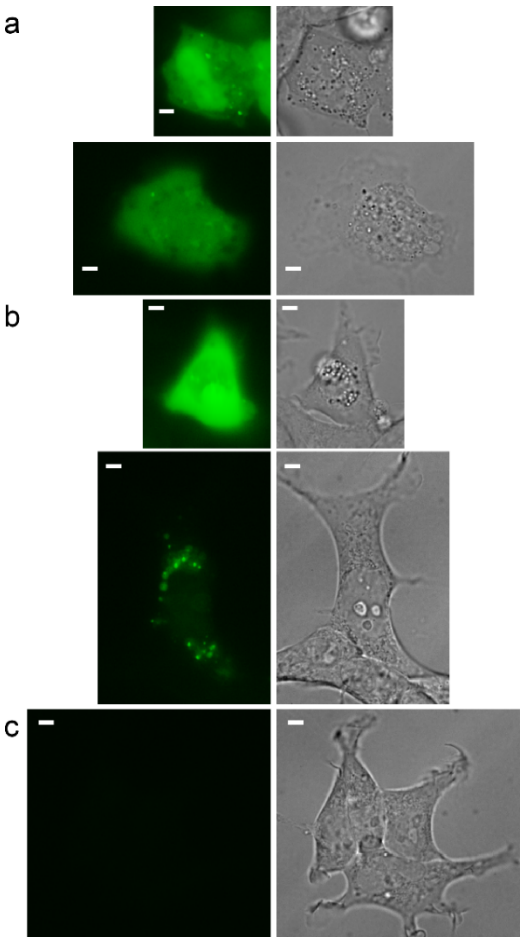

Supplementary Figure 24

Visualization of Broccoli RNA in HEK293T cells using published expression platforms and published imaging conditions. Plasmids pAVU6+27-F30-2xdBroccoli and pAV5S-F30-2xdBroccoli[3] were transfected in HEK293T cells and split into imaging dishes 48 h post transfection following published protocols[3]. 24 h later, DFHBI-1T was added at a final concentration of 40 μM and cells were imaged under widefield illumination conditions as recommended[3]. (a) pAV5S-F30-2xdBroccoli (2 experiments, 14 cells). (b) pAVU6+27-F30-2xdBroccoli. Shown are two representative phenotypes where green fluorescence was either observed diffusely throughout the cell (top) or localized to cytosolic puncta (bottom) (2 experiments, 23 cells). (c) Untransfected control (2 experiments, 32 cells). The brightness and contrast was adjusted to be constant for all images shown. Scale bar = 5 μm.

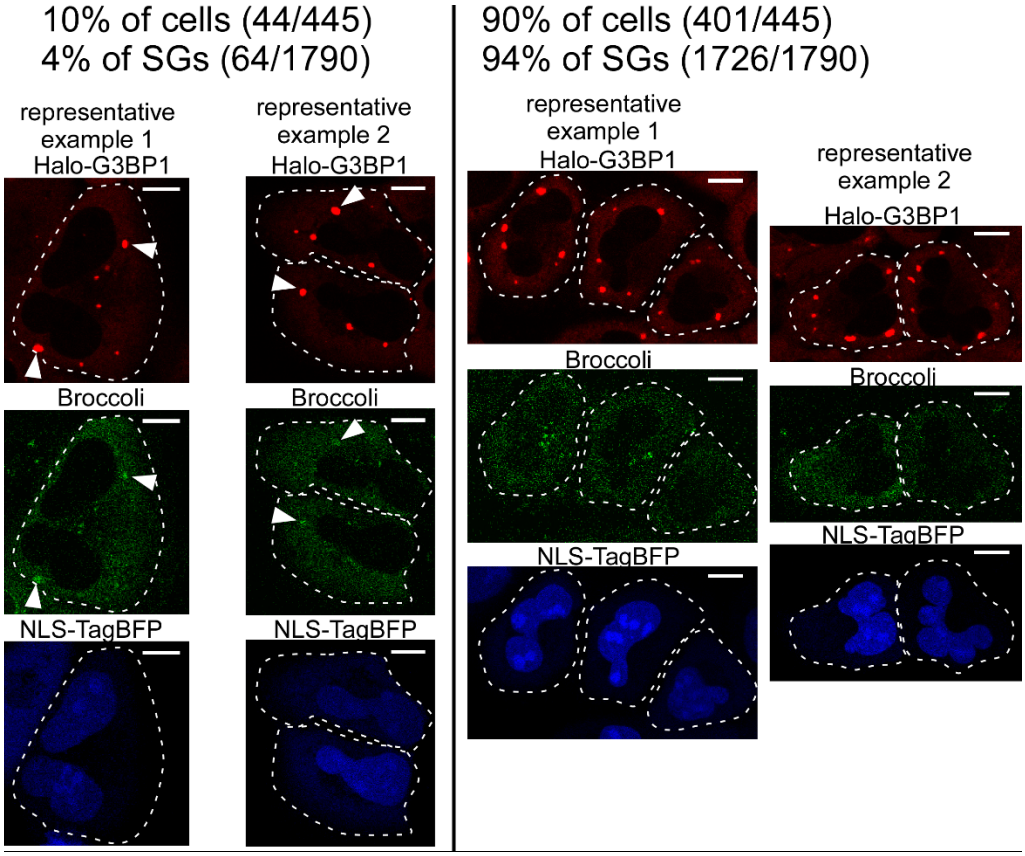

Supplementary Figure 25

Visualization of ACTB mRNA in stress granules (SG) by RNA tagging with Broccoli. ACTB-(2xdBroccoli) was transfected in U2-OS Halo-G3BP1 cells together with the NLS-TagBFP transfection marker. Halo-G3BP1 was labeled with the red fluorescent JF585 dye and SGs were induced by incubation with arsenite for 30-45 min. SGs were identified via the red fluorescent JF585 signal. After addition of the Broccoli probe DFHBI-1T, all cells positive for the blue transfection marker (445 cells, 3 experiments), were assessed for visible SGs in the green Broccoli channel. In 10% of all cells with TagBFP signal, at least one SG was detected in the green channel and overall, 4% of all SGs identified in red were also detected in the green Broccoli channel (1790 SGs total in all 445 cells). Representative SGs visualized by Broccoli are indicated with white arrows. Scale bar = 10 µm.

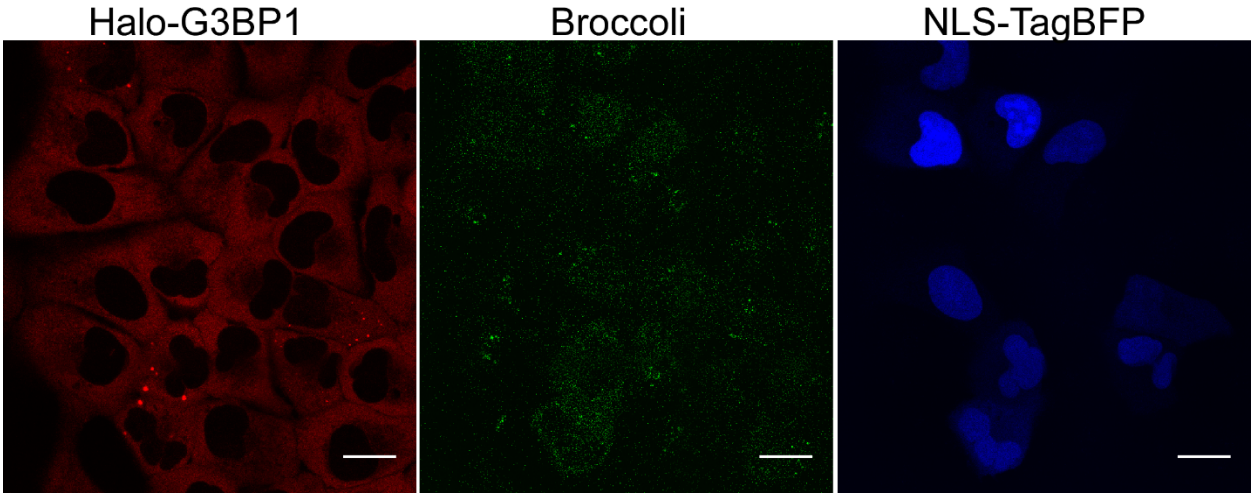

Supplementary Figure 26

Visualization of Broccoli-tagged ACTB mRNA in the absence of arsenite treatment. Plasmids encoding for ACTB-(2xdBroccoli) and the transfection marker NLS-TagBFP were transfected in U2-OS cells. 24 h after transfection, G3BP1 was labeled with the red fluorophore JF585 and the Broccoli dye DFHBI-1T was added. Shown are representative cells. Scale bar = 20 µm.

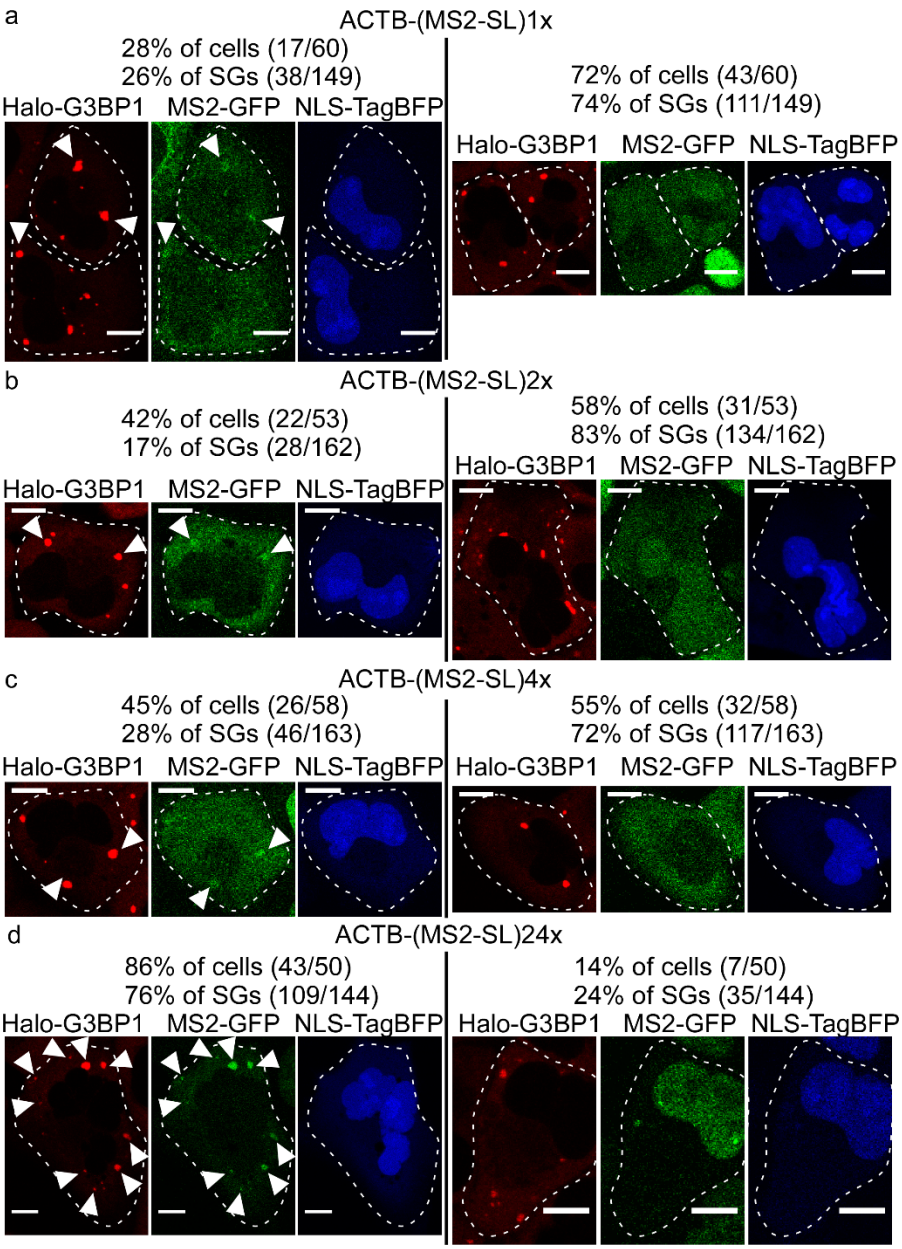

Supplementary Figure 27

Visualization of ACTB mRNA in stress granules (SG) by RNA tagging with MS2 stem-loop (SL) repeats. A plasmid encoding for ACTB tagged with MS2 SL repeats was transfected in U2-OS Halo-G3BP1 cells that stably produce MS2-GFP with the NLS-TagBFP transfection marker. Halo-G3BP1 was labeled with the red fluorescent JF585 dye for SG identification and SGs were induced by arsenite. (a) ACTB-(MS2-SL)1x was transfected (in 28% of all transfected cells at least one SG was detected in the green channel; 38/149 SGs). (b) ACTB-(MS2-SL)2x was

transfected (in 42% of all transfected cells at least one SG was detected in the green channel; 28/162 SGs). (c) ACTB-(MS2-SL)4x was transfected (in 45% of all transfected cells at least one SG was detected in the green channel; 46/163 SGs). (d) ACTB-(MS2-SL)24x was transfected (in 86% of all transfected cells at least one SG was detected in the green channel; 109/144 SGs). Representative SGs visualized by MS2-GFP are indicated with white arrows. Scale bar = 10 μm.

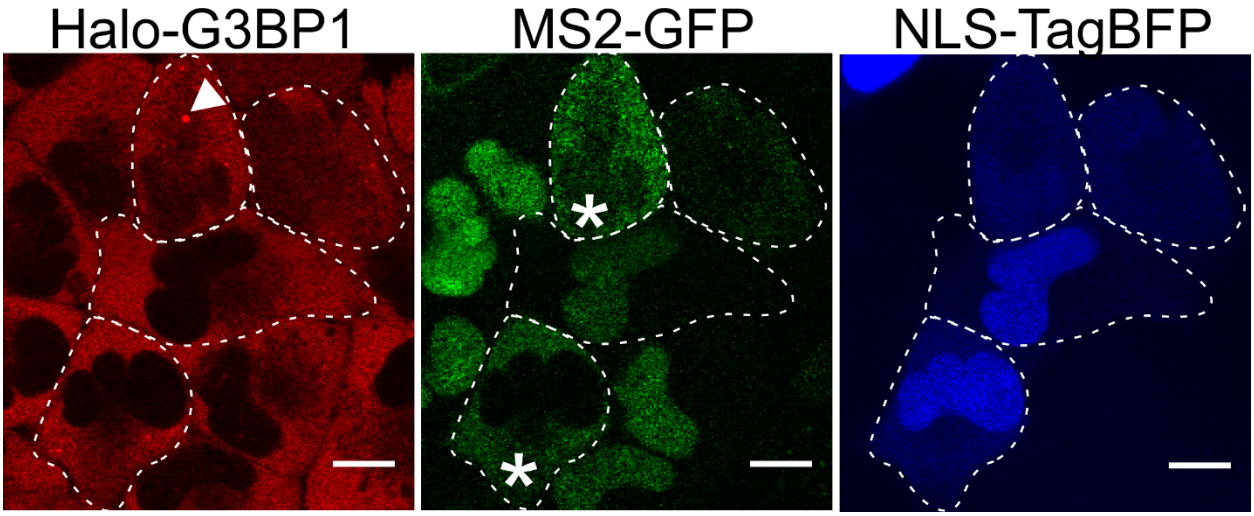

Supplementary Figure 28

Cotransfection of NLS-TagBFP and ACTB-(MS2-SL)24x in U2-OS induces different phenotypes. U2-OS cells that stably produce Halo-G3BP1 and MS2-GFP were cotransfected with plasmid encoding for NLS-TagBFP and ACTB(MS2-SL)24x. 24 h post transfection, G3BP1 was labeled by the red JF585 fluorophore. Cells positive for the NLS-TagBFP transfection marker are indicated by white dashed lines. Untransfected cells as well as some NLS-TagBFP positive cells displayed nuclear MS2-GFP (see for example oval shaped cell in the middle of the field of view). In other cases, MS2-GFP was localized to the cytosol (see cells marked with white stars). Occasionally, stress granules were observed in the red JF585 channel in transfected cells (white arrow).

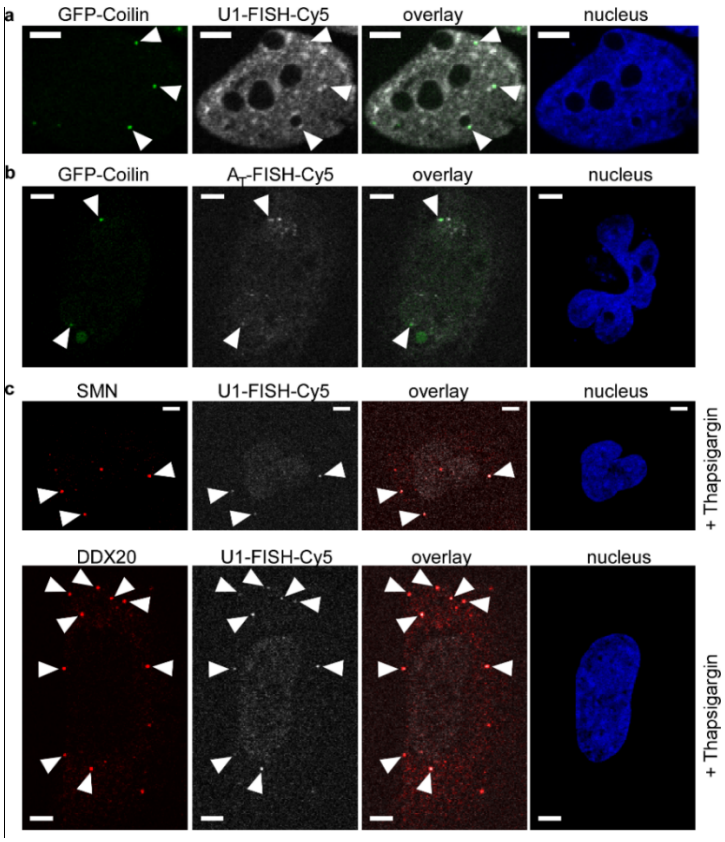

Supplementary Figure 29

Localization phenotypes of U1 snRNA in normal and Thapsigargin-stressed HeLa cells. (a) Endogenous U1 snRNA colocalizes with nuclear Coilin-containing foci. HeLa cells were transiently transfected with a plasmid to produce GFP-Coilin, fixed and permeabilized. U1 snRNA was visualized via a probe against the U1 snRNA coding sequence (1 experiment, 6 cells). (b) A_T-U1 RNA can localize to Coilin-containing nuclear foci. HeLa cells were transiently transfected with two plasmids to produce GFP-Coilin and A_T-U1 snRNA, fixed and permeabilized. A_T-U1 snRNA was visualized via a probe against the A_T aptamer (2 experiments, 3 cells). (c) Endogenous U1 snRNA colocalizes with two marker proteins for U-bodies, endogenous SMN (1 experiment, 5 cells) and endogenous DDX20 (1 experiment, 9 cells), upon Thapsigargin treatment. HeLa cells were fixed and permeabilized. U1 snRNA was visualized via a probe against U1, and DDX20 and SMN were visualized by immunofluorescence. Scale bar = 5 μm.

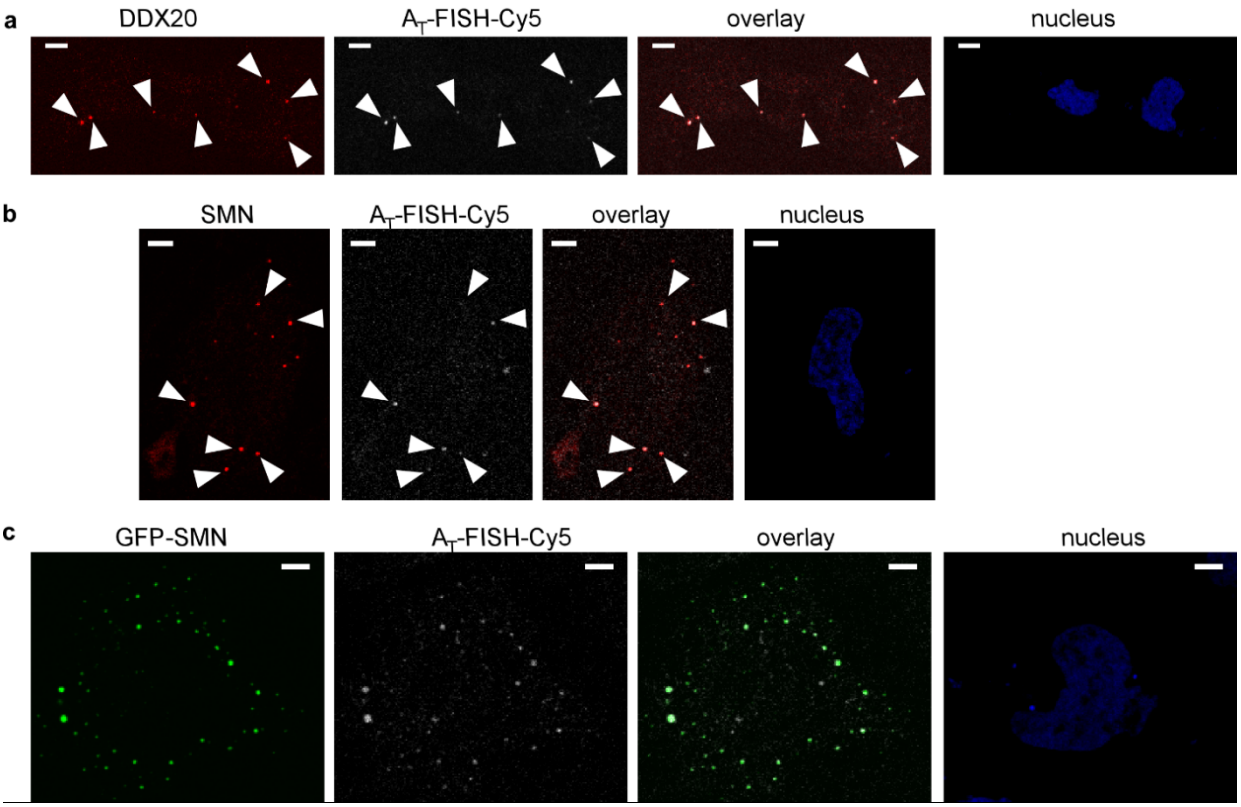

Supplementary Figure 30

Transiently transfected U1 snRNA tagged with A_T can localize to U-body marker proteins DDX20 and SMN. (a) A_T-U1 snRNA can colocalize with the U-body marker protein DDX20 after treatment of cells with Thapsigargin. A_T-U1 snRNA was visualized via an A_T aptamer specific probe and endogenous DDX20 was detected by immunofluorescence (1 experiment, 12 cells). (b) A_T-U1 snRNA can colocalize with the U-body marker protein SMN after treatment of cells with Thapsigargin. A_T-U1 snRNA was visualized via an A_T-specific probe and endogenous SMN was detected by immunofluorescence (1 experiment, 8 cells). (c) A_T-U1 snRNA colocalizes with transiently transfected GFP-SMN after treatment of cells with Thapsigargin. A_T-U1 snRNA was visualized via an A_T-specific probe and SMN was detected by GFP fluorescence (1 experiment, 57 cells). Scale bar = 5 μm.

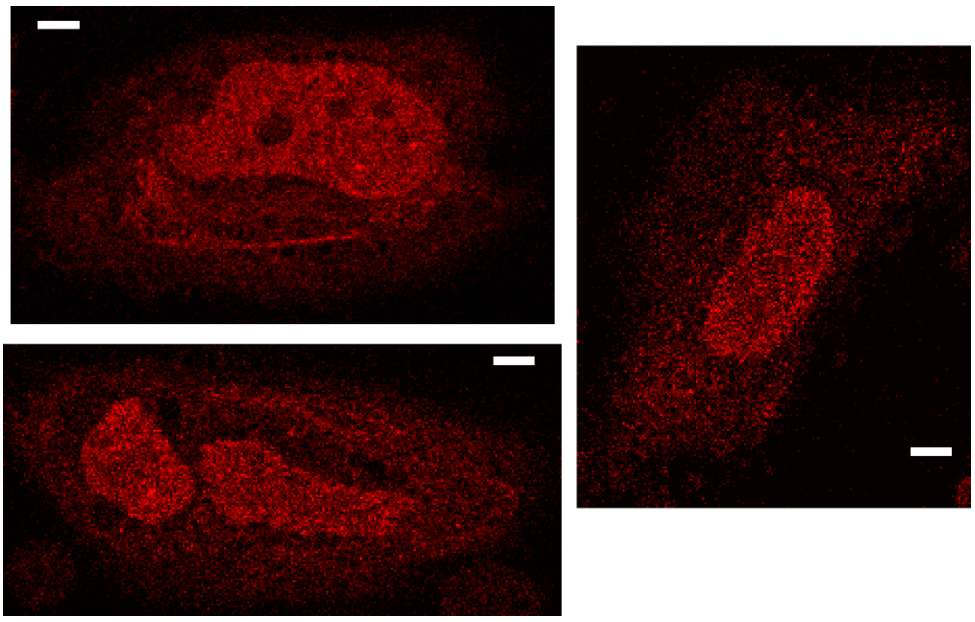

Supplementary Figure 31

In the absence of Thapsigargin-treatment, HeLa cells transfected with A_T-U1 and bead loaded with Cbl-5xPEG-ATTO 590 do not display cytosolic granules resembling U-bodies. HeLa cells were transfected with A_T-U1, bead loaded with Cbl-5xPEG-ATTO 590 24 h later and live microscopy was performed as described in Fig. 5, except that no prior treatment with Thapsigargin was done. Out of 86 cells (1 experiment), 2 cells (2%) displayed cytosolic puncta. Scale bar = 5 µm.

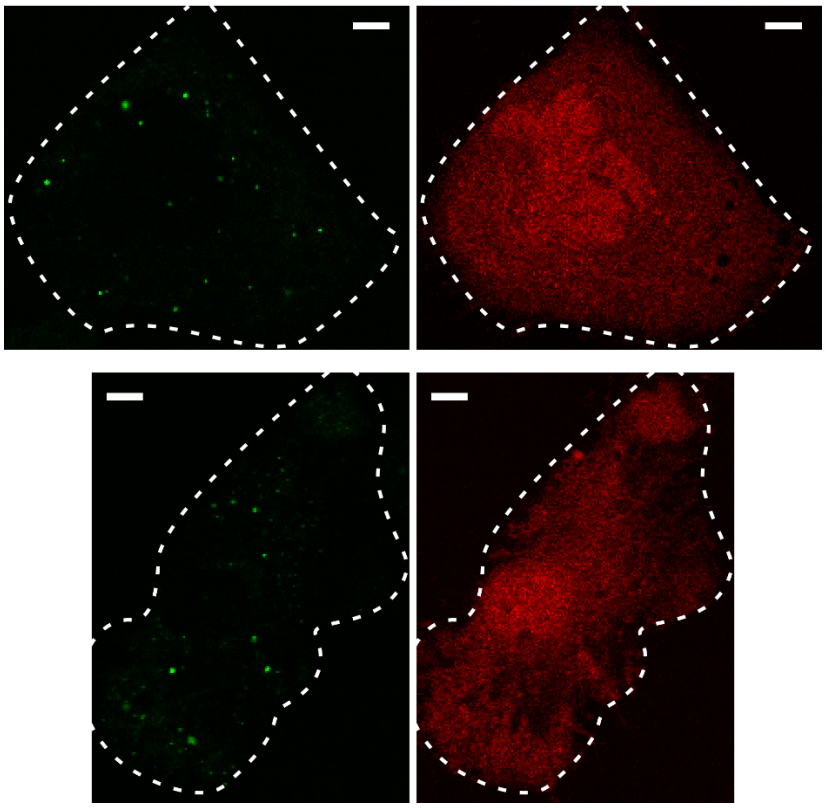

Supplementary Figure 32

Cbl-5xPEG-ATTO 590 does not colocalize to GFP-SMN puncta in the absence of A_T-U1 snRNA. HeLa cells were transiently transfected with a plasmid to produce GFP-SMN, treated with Thapsigargin and loaded with Cbl-5xPEG-ATTO 590. In the absence of a co-transfected plasmid to produce A_T-U1 snRNA, the probe does not accumulate in the puncta marked with GFP (compare with Fig. 5c) (3 experiments, 6 cells). Scale bar = 5 μm.

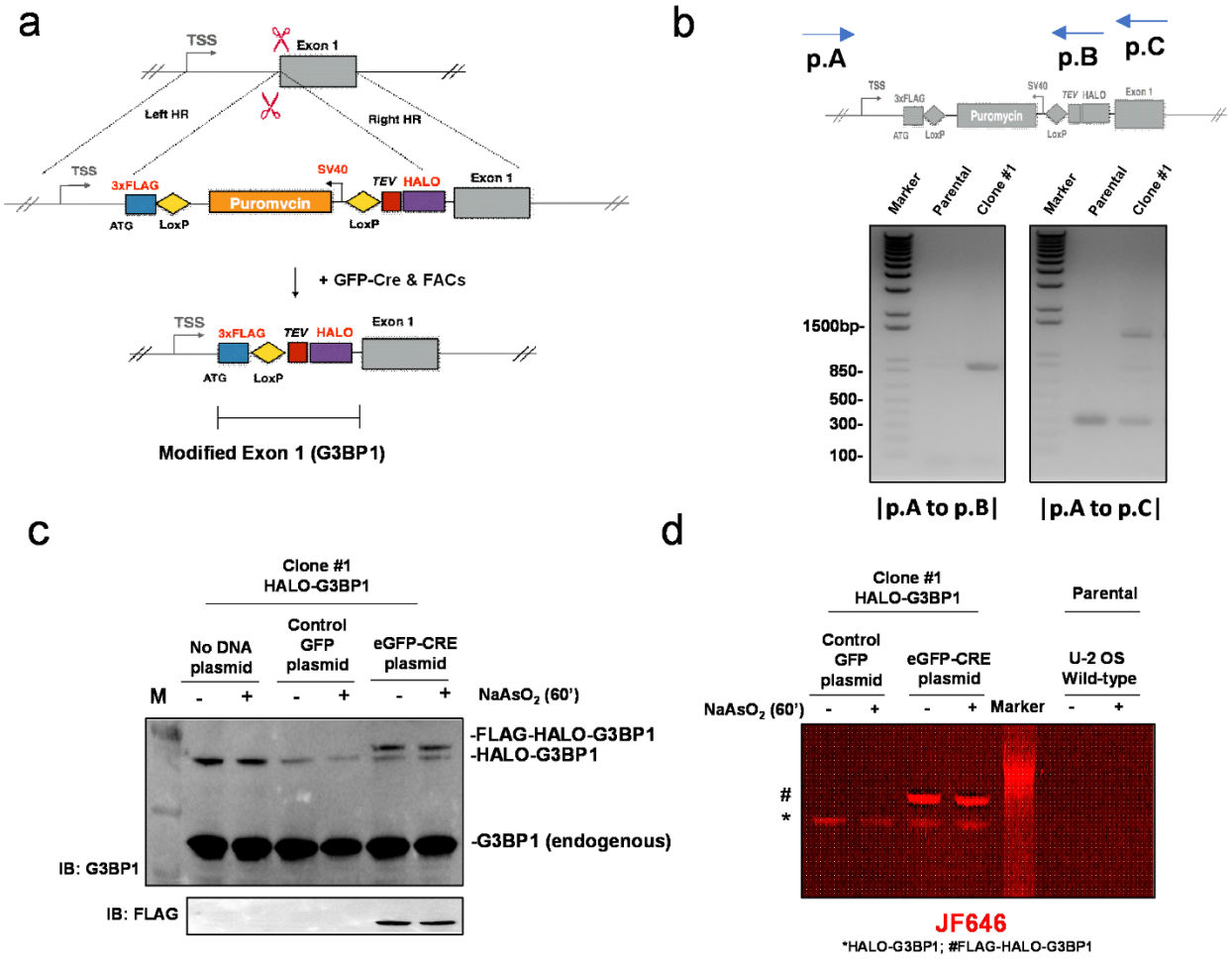

Supplementary Figure 33

Generation of endogenous Halo-G3BP1 cell line. (a) Schematic for CRIPSR/Cas9-mediated 3xFlag-HALO-tag knockin into endogenous G3BP1 locus. (b) Genotyping results reveals

proper integration in mixed U2-OS population. (c) Transient transfection of eGFP-Cre, but not control plasmids, in edited cell reveals correct expression of 3xFlag-HALO-tagged G3BP1 resolved by Western blotting. (d) Same as (c) expect 3xFlag-Halo-tag integration at the G3BP1 locus resolved by fluorescent imaging of protein gels. (e) 3xFlag-Halo-tagged G3BP1, as resolved by different fluorescent dyes, redistributes from the cytoplasm to concentrate into stress granules during sodium arsenite stress. Scale bar = 5 μm.

Supplementary Tables

Supplementary Table 1

Photophysical properties of fluorophores, probes and Cbl.

Name	Extinction coefficient ε [L mol^{-1} cm^{-1}] (source)	Excitation λ	Emission range
FAM	80,000 (490 nm) (Lumiprobe)	488 nm	503 - 660 nm
Cbl-FAM	80,000 (490 nm) (Lumiprobe)	488 nm	503 - 660 nm
Cbl-C6-FAM	80,000 (490 nm) (Lumiprobe)	488 nm	503 - 660 nm
Cbl-1xPEG-FAM	80,000 (490 nm) (Lumiprobe)	488 nm	503 - 660 nm
Cbl-2xPEG-FAM	80,000 (490 nm) (Lumiprobe)	488 nm	503 - 660 nm
Cbl-3xPEG-FAM	80,000 (490 nm) (Lumiprobe)	488 nm	503 - 660 nm
ATTO 488	90,000 (501 nm) (Atto tec)	501 nm	511 - 700 nm
Cbl-C6-ATTO488	90,000 (501 nm) (Atto tec)	501 nm	511 - 700 nm
ATTO 590	120,000 (594 nm) (Atto tec)	594 nm	604 - 820 nm
Cbl-ATTO 590	120,000 (594 nm) (Atto tec)	594 nm	604 - 820 nm
Cbl-C6-ATTO 590	120,000 (594 nm) (Atto tec)	594 nm	604 - 820 nm
Cbl-5xPEG-ATTO 590	120,000 (594 nm) (Atto tec)	594 nm	604 - 820 nm
Cbl-5xGly-ATTO 590	120,000 (594 nm) (Atto tec)	594 nm	604 - 820 nm
ATTO 633	130,000 (629 nm) (Atto tec)	629 nm	639 - 850 nm
Cbl-ATTO 633	130,000 (629 nm) (Atto tec)	629 nm	639 - 850 nm
Cbl-C6-ATTO 633	130,000 (629 nm) (Atto tec)	629 nm	639 - 850 nm
Cy5	271,000 (646 nm) (Lumiprobe)	646 nm	656 - 800 nm
Cbl-Cy5	271,000 (646 nm) (Lumiprobe)	646 nm	656 - 800 nm
Cbl	27,642.26 (361 nm)		

Supplementary Table 2

Theoretical estimates of parameters for energy transfer between Cbl absorbance and fluorescence emission of each fluorophore.

Fluorophore	Overlap integral J(λ) between fluorescence emission and Cbl absorbance	Quantum yield Q of fluorophore (source)	Förster distance R_0
FAM	1.374 x 10^{14} nm^4 M^{-1} cm^{-1}	0.93 (Lumiprobe)	35 Å
ATTO 488	1.424 x 10^{14} nm^4 M^{-1} cm^{-1}	0.80 (Atto tec)	35 Å
ATTO 590	5.266 x 10^{12} nm^4 M^{-1} cm^{-1}	0.80 (Atto tec)	20 Å
ATTO 633	1.026 x 10^{12} nm^4 M^{-1} cm^{-1}	0.64 (Atto tec)	15 Å
Cy5	7.638 x 10^{11} nm^4 M^{-1} cm^{-1}	0.28 (Lumiprobe)	12 Å

Supplementary Table 3

Estimates of linker lengths.

Name of linker	**Estimated length (values for PEG linkers published by ThermoFisher Scientific)**
C6	10.5 Å (estimated to be similar to 3xPEG)
1xPEG	3.5 Å
2xPEG	7.0 Å
3xPEG	10.5 Å
5xPEG	17.5 Å
5xGly	21.4 Å (Berg, Tymoczko & Stryer, Biochemisty, 2002)

Supplementary Table 4

Summary of fold on turn-on for Cbl-fluorophore probes in the presence of aptamers (Fig. 2)

Name of Cbl-fluorophore probe	**Name of aptamer**	**Fold fluorescence turn on**
Cbl-FAM	$A_{T,MUT}$	0.5x
	A_T	2.5x
Cbl-C6-FAM	$A_{T,MUT}$	1.1x
	A_T	4.1x
Cbl-3xPEG-FAM	$A_{T,MUT}$	1.1x
	A_T	2.8x
	B	7.4x
Cbl-C6-ATTO 488	$A_{T,MUT}$	1.1x
	A_T	1.3x
Cbl-C6-ATTO 590	$A_{T,MUT}$	1.2x
	A_T	2.9x
	B	3.9x
Cbl-5xPEG-ATTO 590	$A_{T,MUT}$	1.1x
	A_T	4.0x
	A	4.9x
	B	3.7x
	C	4.0x
	D	2.9x
Cbl-5xGly-ATTO 590	A_T	7.3x
	A	5.0x
	D	3.9x

Cbl-C6-ATTO 633	$A_{T,MUT}$	0.9x
	A_T	1.9x
	B	2.5x
Cbl-Cy5	$A_{T,MUT}$	1.1x
	A_T	2.1x
	A	2.7x
	B	2.5x
	D	2.5x

Supplementary Table 5

Comparison of maximal distance between the corrin ring in Cbl and the fluorophore in probes. Values are based on structural estimates and the Förster distance R_0 estimated from spectral properties.

Name	Distance estimate between corrin ring and click linkage to fluorophore	Förster distance R_0
Cbl-FAM	9 Å	
Cbl-C6-FAM	12.5 Å	
Cbl-1xPEG-FAM	12.5 A	35 Å
Cbl-2xPEG-FAM	16 Å	
Cbl-3xPEG-FAM	19.5 Å	
Cbl-C6-ATTO488	12.5 Å	35 Å
Cbl-ATTO 590	9 Å	
Cbl-C6-ATTO 590	12.5 Å	
Cbl-5xPEG-ATTO 590	26.5 Å	20 Å
Cbl-5xGly-ATTO 590	30.4 Å	
Cbl-ATTO 633	9 Å	
Cbl-C6-ATTO 633	12.5 Å	15 Å
Cbl-Cy5	9 Å	12 Å

Supplementary Table 6

Summary of ITC titrations for different aptamers in the presence of Cbl or the Cbl-5xPEG-ATTO 590 probe.

Name of aptamer	Name of conjugate	K_D
A	Cbl	37 ± 1 nM
A	Cbl-5xPEG-ATTO 590	34 ± 9 nM
A_T	Cbl	290 ± 100 nM
A_T	Cbl-5xPEG-ATTO 590	1.3 ± 0.56 µM
D	Cbl	2.2 ± 1.6 nM
D	Cbl-5xPEG-ATTO 590	3.0 ± 0.6 nM

All measurements were done in triplicates and values are reported as the mean ± STDEV.

Supplementary Table 7

Quantum yield of probes in the presence and absence of different aptamers.

Name	Quantum yield (QY)
Cy5	0.28 (Lumiprobe)
Cbl-Cy5	0.09
Cbl-Cy5 + A	0.26
Cbl-Cy5 + D	0.25
ATTO 590	0.8 (Atto Tec)
Cbl-5xPEG-ATTO 590	0.06
Cbl-5xPEG-ATTO 590 + A	0.31
Cbl-5xPEG-ATTO 590 + D	0.31
Cbl-5xGly-ATTO 590	0.09
Cbl-5xGly-ATTO 590 + A	0.55
Cbl-5xGly-ATTO 590 + D	0.45

Supplementary Table 8

Summary of fluorescence lifetime measurements for Cbl-fluorophore probes in the presence and absence of indicated aptamers. The lifetime decay data presented in Supplementary Fig. 10 was fit and exponential components and their weight are indicated together with the overall fluorescence lifetime.

	t_1 (ns)	**t_1 %**	**t_2 (ns)**	**t_2 %**	**t_3 (ns)**	**t_3 %**	**lifetime (ns)**
Cy5	1.04	100					**1.04**
Cbl-Cy5	0.33	25	0.7	75			**0.61**
Cbl-Cy5 + D	1	100					**1**
Cbl-Cy5 + A	1.05	100					**1.05**
ATTO 590	3.99	100					**3.99**
Cbl-5xGly-ATTO 590	0.2	9	0.89	32	1.94	59	**1.44**
Cbl-5xGly-ATTO 590 + D	0.4	6	1.75	46	3.3	48	**2.42**
Cbl-5xGly-ATTO 590 + A	0.43	5	1.84	33	3.79	62	**2.98**
Cbl-5xPEG-ATTO 590	0.25	28	1.56	72			**1.19**
Cbl-5xPEG-ATTO 590 + D	0.4	12	1.61	60	3.22	28	**1.93**
Cbl-5xPEG-ATTO 590 + A	0.41	13	1.42	43	3.34	44	**2.14**

Supplementary Table 9

Experimental conditions for RNA / probe photobleaching experiments.

Probe	RNA	Excitation wavelength (nm)	Irradiance (W/cm^2)
55 µM Cbl-Cy5	550 µM A	640	0.27
48 µM Cbl-5xPEG-ATTO 590	480 µM A	555	1.31
7 µM DFHBI-1T	80 µM Broccoli	470	3.16

Supplementary Table 10

Sequence and properties of DNA oligos used in FISH.

Name	Sequence	Melting temperature (IDT)	amount per cover slip
ACTB-FISH-Cy5	5'-Cy5-CAC AGC TTC TCC TTA ATG TCA CGC ACG ATT TCC CGC TCG GCC GTG-3'	71.1°C	300 ng
A_T-FISH-Cy5	5'-Cy5-CCT AGG TGG CAT TCG GAG TAT AAC CGT ATC AAG TAA TCT G-3'	63.3°C	200-300 ng
A_T-FISH-Alexa546	5'-Alexa546-CCT AGG TGG CAT TCG GAG TAT AAC CGT ATC AAG TAA TCT G-3'	63.3°C	300 ng
Broccoli-FISH-Cy5	5'-Cy5-TTG CCA TGA ATG ATC CAG CCC ACA CTC-3'	62.8°C	300 ng
MS2SL-FISH-Cy5	5'-Cy5-GTT TAA ACG AAT TCG CCC TTA GAT CTG ATG AAC CCT GG-3'	63.5°C	300 ng
U1-FISH-Cy5	5'-Cy5-TCA GCA CAT CCG GAG TGC AAT GGA TAA GCC TCG CCC TGG GAA AA-3'	71.3°C	200-300 ng

References

1. Johnson, J. E., Reyes, F. E., Polaski, J. T. & Batey, R. T. B12 cofactors directly stabilize an mRNA regulatory switch. *Nature* **492,** 133–7 (2012).

2. Polaski, J. T., Webster, S. M., Johnson, J. E. & Batey, R. T. Cobalamin Riboswitches Exhibit a Broad Range of Ability to Discriminate between Methylcobalamin and Adenosylcobalamin. *J. Biol. Chem.* **292,** 11650–11658 (2017).

3. Filonov, G. S. & Jaffrey, S. R. *RNA Imaging with Dimeric Broccoli in Live Bacterial and Mammalian Cells*. *Current protocols in chemical biology* **8,** (2016).